climate

MDPI

Article

Quantifying Local Climate Change Through Statistical Downscaling: A Case Study of the Canagagigue Creek Watershed, Canada

Rong Hu [1], Ramesh P. Rudra [1], Ashok Shaw [2], Rituraj Shukla [1,*] and Pradeep Goel [3]

[1] College of Engineering, University of Guelph, Guelph, ON N1G 2W1, Canada; lhu@stantec.com (R.H.); rrudra@uoguelph.ca (R.P.R.)
[2] School of Environmental Sciences, University of Guelph, Guelph, ON N1G 2W1, Canada; ashaw20@uoguelph.ca
[3] Ontario Ministry of the Environment, Conservation, and Parks, Etobicoke, ON M9P 3V6, Canada; pradeep.goel@ontario.ca
* Correspondence: rshukla@uoguelph.ca; Tel.: +1-5197315910

Abstract

This study investigates historical and future climate variability in the Canagagigue Creek Watershed, located in southern Ontario, through statistical downscaling and trend assessment of key climate variables. Future climate projections from the Canadian Global Circulation Model (CGCM2) under SRES A2 and B2 emission scenarios were downscaled using the Statistical Downscaling Model (SDSM) to generate daily maximum temperature (T_{max}), minimum temperature (T_{min}), and precipitation series for the future period of 2025 to 2044. Historical observations were used to calibrate (1961–1990) and validate (1991–2001) SDSM performance as well as to evaluate long-term trends in local climate conditions. Results indicate that SDSM provides better downscaling performance for temperature variables than for precipitation, with reliable reproduction of historical T_{max} and T_{min} patterns (NSE > 0.98). Downscaled future projections suggest consistent warming across the watershed, characterized by warmer winters and hotter summers, along with reduced temperature variability. Historical trend analysis reveals significant increases only in T_{min} (0.033 °C per decade, $p = 0.076$), while T_{max} and precipitation trends show weak or statistically insignificant changes. Future trends similarly indicate notable increases in T_{min}, particularly during winter months (up to 0.13 °C per decade, $p < 0.05$), whereas changes in mean precipitation (P_{mean}) remain minimal. Increased summer precipitation variability, however, suggests a greater likelihood of heavy rainfall events, albeit with large uncertainty. Overall, this study demonstrates the utility of statistical downscaling for generating watershed-scale climate information and provides insight into evolving temperature and precipitation patterns that may influence environmental and resource management planning in southern Ontario.

Keywords: statistical downscaling; SDSM; CGCM2; climate projections; southern Ontario

Check for updates

Received: 6 May 2026
Revised: 30 June 2026
Accepted: 14 July 2026
Published: 17 July 2026

1. Introduction

Over the last century, the impacts of climate change have become increasingly evident across both natural and human-influenced environments. These changes are affecting atmospheric processes worldwide [1]. The Sixth Assessment Report of the Intergovernmental Panel on Climate Change (IPCC) shows that the Earth's average surface temperature during the last two decades was approximately 1.1 °C higher than during the pre-industrial period (1900s). The report clearly states that this warming is unequivocal. It also confirms that human activities, particularly rising greenhouse gas concentrations in the atmosphere, are the primary cause of this long-term warming trend [2]. While global- and continental-scale assessments provide essential evidence of climate change, their utility for decision-making depends on the translation of broad-scale climate signals into locally relevant information. This scale dependency highlights a fundamental challenge in climate science: reconciling global climate projections with local environmental processes that directly influence water resources, ecosystems, and land management [1].

The need for localized climate assessment is particularly acute at the watershed scale, where climatic variability directly governs hydrological behavior, sediment transport, and water quality [3,4]. Watersheds represent the primary spatial unit for water-resource management, linking climate forcing with land use, soil characteristics, and ecological responses. In southern Ontario, watersheds support highly productive agricultural systems, dense population centers, and ecologically sensitive aquatic environments [5–7]. In recent decades, the region has experienced increasing climate-related impacts, including more frequent flooding associated with intense rainfall events, prolonged summer dry periods and droughts affecting agricultural production, warmer winters with reduced snow cover, and more frequent freeze–thaw cycles [5,8]. These trends are projected to intensify under future climate scenarios, altering seasonal water balances, increasing evapotranspiration, and amplifying both flood and drought risks [9,10]. Consequently, high-resolution, watershed-scale climate information is essential for effective environmental and water-resource planning in southern Ontario.

Global Climate Models (GCMs) remain the cornerstone of future climate projection, simulating climate system responses to varying greenhouse gas emission scenarios based on assumptions about population growth, economic development, and energy use [2,11]. Models such as the Canadian Global Climate Model version 2 (CGCM2) have been widely applied to project future temperature and precipitation under IPCC Special Report on Emissions Scenarios (SRES), including the A2 and B2 pathways [11]. However, GCMs operate at coarse spatial resolutions, typically exceeding 100 km, which limits their ability to capture local climate variability, extremes, and site-specific influences such as land-use heterogeneity, topography, and proximity to large water bodies [12,13]. Numerous studies have shown that direct application of GCM outputs at local scales often results in biased representations of daily temperature and precipitation patterns, particularly for extreme events critical to environmental impact assessments [14,15].

To overcome these limitations, downscaling approaches have become essential for translating coarse-resolution GCM projections into locally relevant climate information [13,16]. Statistical downscaling methods establish empirical relationships between large-scale atmospheric predictors and local surface climate variables, enabling the generation of site-specific, high-resolution daily climate time series [12]. Compared to dynamical downscaling using Regional Climate Models, statistical approaches are computationally efficient, flexible, and well suited for studies requiring multiple scenarios and long-term simulations [17]. Recent studies demonstrate that statistical downscaling can reliably reproduce historical climate characteristics when appropriately calibrated, particularly for temperature variables, while precipitation remains more uncertain due to its inherent spatial and temporal variability [18,19].

Among available statistical downscaling tools, the Statistical Downscaling Model (SDSM) is one of the most widely applied and well-documented frameworks, especially in Canadian climate studies [12,16,20]. SDSM combines multiple linear regression with a stochastic weather generator to simulate daily maximum temperature (T_{max}), minimum temperature (T_{min}), and precipitation based on large-scale atmospheric predictors derived from GCMs. Its transparency, modest data requirements, and compatibility with Canadian climate datasets have contributed to its extensive use in regional and watershed-scale applications across Canada [21,22]. Continued methodological refinements have further strengthened its relevance for contemporary climate assessments, including improved predictor selection, bias correction, and representation of climate variability [17,23]. Alternative downscaling approaches include dynamical downscaling using Regional Climate Models (RCMs) and more recent machine learning (ML) methods (e.g., random forests, deep learning). RCMs provide physically consistent outputs but are computationally expensive and require substantial expertise. ML methods can capture non-linearities but often lack interpretability and require large training datasets. SDSM was selected for this study because it is transparent, computationally efficient, well-documented for Canadian climates, and possesses attributes well-suited for a watershed-scale impact assessment.

While more recent Global Climate Models from CMIP5 and CMIP6 are now standard for climate projections, this study employs the Canadian Global Climate Model version 2 (CGCM2) under the SRES A2 high-emission scenario for three primary reasons. First, CGCM2 provides a well-established benchmark that has been widely used in earlier Canadian watershed studies (e.g., Bonsal et al., [24]; Dibike & Coulibaly, [25]), allowing direct methodological comparison and continuity with prior regional impact assessments. Second, the principal objective of this study is to develop and rigorously validate a statistical downscaling approach (SDSM) for generating reliable, watershed-scale daily climate series, rather than to provide a multi-model ensemble projection. Using a single, well-documented climate model ensures clarity in evaluating downscaling performance and trend characteristics without introducing inter-model variability that would obscure the assessment of the downscaling method itself. Third, the climate change signals identified in this study, including consistent warming, particularly in minimum temperature, changes in seasonal variability, and altered precipitation patterns, are broadly consistent with findings from more recent CMIP5- and CMIP6-based studies in southern Ontario [26,27]. This agreement suggests that the directional trends reported here are robust, even though the absolute magnitudes may be refined with newer models.

Recent applications of SDSM and related statistical downscaling approaches reinforce both their strengths and limitations. Multiple studies indicate that downscaled temperature variables, particularly T_{min}, exhibit strong agreement with observed trends, whereas precipitation projections show greater uncertainty and weaker statistical significance [28,29]. Similar findings have been reported across diverse climatic regions, emphasizing the importance of localized evaluation of downscaled outputs prior to application in impact and planning studies [14,19].

Despite the widespread use of SDSM and the availability of CGCM-based projections, a notable research gap persists. Localized climate trend assessments for small watersheds in southern Ontario remain limited, particularly those integrating long-term historical trend analysis with statistically downscaled CGCM projections at daily resolution [7,10]. Many existing studies focus on regional or basin-scale analyses, providing limited insight into fine-scale climate variability and seasonal trends that are critical for watershed-specific environmental management. While SDSM has been applied in many Canadian studies, very few have combined a multi-decadal historical probability density function (PDF) trend analysis with downscaled projections for a small agricultural watershed. Moreover, most previous work focused on mean changes; this study explicitly examines changes in variability, extremes, and spell lengths. These features provide new, locally relevant insights for water quality and erosion management in southern Ontario.

Within this context, the Canagagigue Creek Watershed, a sub-watershed of the Grand River in southern Ontario, Canada, provides a representative case study. The watershed's intensive agricultural land use, documented water quality concerns, and sensitivity to hydroclimatic variability highlight the need for localized, high-resolution climate information to support adaptive planning and management [3,6].

Accordingly, this study seeks to address the identified research gap by conducting a localized climate change assessment using a statistical downscaling approach. The specific objectives are: (1) to evaluate historical trends (1940–2003) in daily maximum temperature (Tmax), minimum temperature (Tmin), and precipitation within the Canagagigue Creek Watershed; (2) to downscale CGCM2 climate projections under the SRES A2 and B2 emission scenarios over a 30-year period, including 10 years (2015–2024) for model verification and 20 years (2025–2044) for future projections, using the Statistical Downscaling Model (SDSM); (3) to assess projected changes for 2025–2044 by presenting confidence and prediction interval analyses to illustrate variability in temperature and precipitation at the watershed scale. By combining historical trend analysis with statistically downscaled climate projections, this study provides reliable, watershed-scale climate insights to support environmental management and water resource planning in southern Ontario.

2. Study Area and Data

2.1. Description of Study Area

The Canagagigue Creek Watershed (CCW) is located in southern Ontario, Canada, near the community of Floradale, and forms part of the upper Grand River Basin. The watershed lies between latitudes 43°36′ N and 43°42′ N and longitudes 80°33′ W and 80°38′ W and drains an area of approximately 53 km^2 [30,31]. The large-scale atmospheric predictor variables were extracted from the nearest grid cells of the NCEP reanalysis and HadCM3 GCM datasets. The NCEP reanalysis data were available at a spatial resolution of 2.5° latitude × 2.5° longitude, corresponding to an approximate regional coverage of 278 km × 203 km over southern Ontario. Similarly, the HadCM3 GCM predictors were available at a spatial resolution of 2.5° latitude × 3.75° longitude, representing an approximate grid size of 278 km × 304 km in the study region. These large-scale predictor grids represent synoptic atmospheric conditions and were extracted from the nearest grid cells centered at 42.5° N, 80.0° W (NCEP) and 42.5° N, 78.75° W (HadCM3) relative to the centroid of the Canagagigue Creek Watershed (43.39° N, 80.58° W) [15]. Flow from the watershed ultimately contributes to the Grand River, one of the most significant river systems in Ontario, which discharges into Lake Erie. The spatial extent of the watershed and its location within the Grand River Basin are shown in Figure 1.

Topographically, the Canagagigue Creek Watershed is characterized by low relief, with an average elevation of approximately 417 m above sea level and gentle slopes generally less than 1.5%. Although the watershed has low topographic relief, minor spatial heterogeneity in temperature and precipitation may arise from variations in land cover (agriculture vs. forest), soil moisture, and distance from the Great Lakes (approximately 100 km to Lake Erie). This subdued terrain reflects the glacial history of southern Ontario and influences runoff generation, drainage density, and sediment transport processes. Soils within the watershed are predominantly loam and silt loam, with smaller areas of sandy loam, derived from glacial till and lacustrine deposits [32,33]. These soil textures exhibit moderate permeability and erodibility, making the watershed responsive to changes in precipitation intensity and seasonal moisture conditions.

The climate of the CCW is continental humid, with cold winters and warm summers typical of southern Ontario. The mean annual air temperature is approximately 6.5 °C, and precipitation is distributed throughout the year, with snowfall contributing signifi-

https://doi.org/10.3390/cli14070150

cantly to winter moisture storage and spring runoff [31]. Annual evaporation accounts for roughly 65% of total precipitation, reflecting the balance between climatic demand and land-surface processes. As a result, the watershed is sensitive to interannual climate variability, particularly shifts in temperature, snowfall, and rainfall intensity.

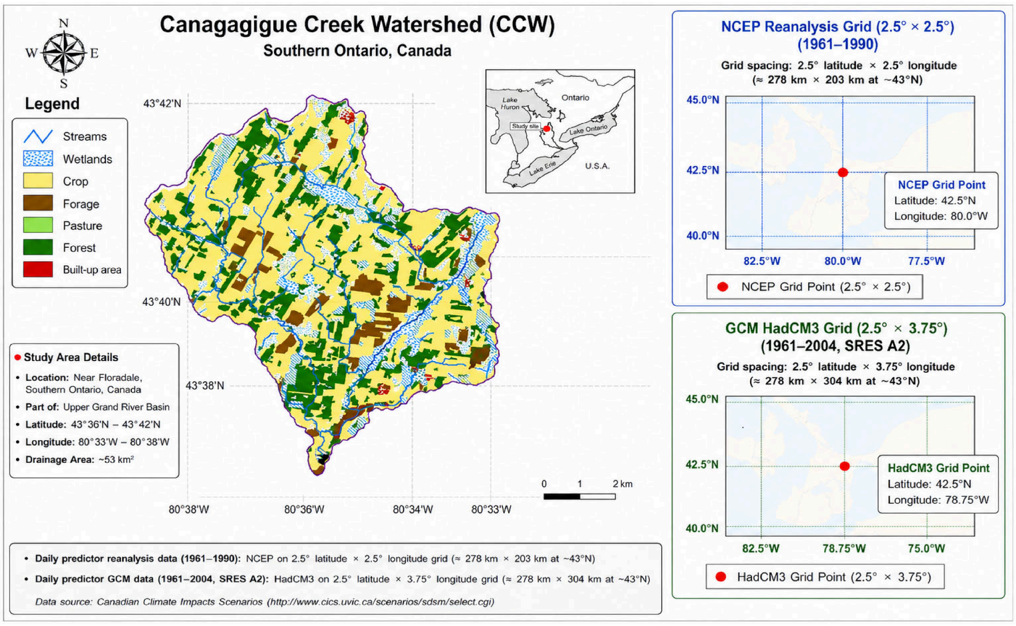

Figure 1. Location of the Canagagigue Creek Watershed.

Land use within the Canagagigue Creek Watershed is dominated by agriculture, which occupies approximately 80% of the total area. Major crops include soybean, corn, and winter wheat, with additional areas of hay and pasture. Forested land covers about 11% of the watershed, while wetlands, residential areas, and open water constitute a minor fraction [30,31]. The distribution of land use and soil types is presented in Supplementary (S1), Figure S1.

The predominance of agricultural land use, combined with gently sloping terrain and moderately erodible soils, has important hydrological and environmental implications. Previous studies have identified the CCW as a significant contributor of sediment and nutrients, particularly nitrogen and phosphorus, to the Grand River system [3,6,21]. These characteristics make the Canagagigue Creek Watershed a representative and environmentally important case study for assessing localized climate variability and its implications for watershed management in southern Ontario.

2.2. Climate Data

Observed daily climate data were used for statistical downscaling, calibration, validation, and historical climate characterization. The variables considered include daily maximum temperature (T_{max}), daily minimum temperature (T_{min}), and daily mean precipitation (P_{mean}). These data were obtained for the Fergus climate station in southern Ontario from the archived Canadian Daily Climate Data (CDCD) database maintained by Environment and Climate Change Canada. The observational record spans 1940–2003, providing a long-term dataset suitable for baseline characterization and trend analysis, consistent with established downscaling studies [16]. According to the World Meteorological Organization (WMO), climate studies generally use at least 30 years of data (for example, 1961–1990). This is because climate describes the long-term average pattern of weather, not short-term changes from year to year. Using a 30-year period helps smooth out temporary ups and downs in temperature or rainfall and provides a reliable baseline for comparing climate trends across different regions and time periods [25].

Prior to their application in the Statistical Downscaling Model (SDSM), the observed datasets were subjected to quality control procedures. Screening included checks for missng values, unrealistic extremes, and internal consistency between temperature variables. Additional assessment was conducted using the SDSM Quality Control module, which permits limited missing data in observed predictands. For the period used in SDSM calibration (1961–1990) and validation (1991–2001), the proportion of missing data was very small: 0.16% for daily T_{max}, 0.13% for daily T_{min}, and 0.13% for daily P_{mean}. Given these low percentages, no infilling was applied, and uncertainties related to data gaps were considered negligible. A summary of data availability and missing records is provided in Table 1.

Table 1. Summary of observed climate data and missing records used in SDSM.

Variable	Data Length Observed	Data Length Downscaled	Missing Data (Days)	Source	Remarks
T_{max}	(1961–1990), calibration and (1991–2001) validation periods	1961–2002 (baseline) and 2015–2044 (downscaled)	24	Canadian Daily Climate Data (CDCD), Environment and Climate Change Canada	0.16% of observed data missing during 1961–2002; downscaled series generated by SDSM contains no missing values
T_{min}	(1961–1990) calibration and (1991–2001) validation periods	1961–2002 (baseline) and 2015–2044 (downscaled)	21	Canadian Daily Climate Data (CDCD), Environment and Climate Change Canada	0.13% of observed data missing during 1961–2002; downscaled series generated by SDSM contains no missing values
P_{mean}	(1961–1990), calibration and (1991–2001) validation periods	1961–2002 (baseline) and 2015–2044 (downscaled)	20	Canadian Daily Climate Data (CDCD), Environment and Climate Change Canada	0.13% of observed data missing during 1961–2002; downscaled precipitation series generated by SDSM contains no missing values

Large-scale atmospheric predictor variables required for downscaling were derived from the Canadian Global Circulation Model version 2 (CGCM2), developed by the Canadian Center for Climate Modeling and Analysis. Global Circulation Models have been widely applied for future climate projection since the 1990s, typically using 1961–1990 as the baseline climatological period [16,25]. CGCM2 operates at a coarse spatial resolution of approximately 3.75° × 3.75°, corresponding to grid dimensions of about 417 km × 342 km over southern Ontario [34], which necessitates statistical downscaling for station-scale applications.

CGCM2 provides climate projections under multiple Special Report on Emissions Scenarios (SRES), including A2 and B2, as documented by the Canadian Climate Change Scenarios Network [35]. The A2 scenario represents a heterogeneous, regionally focused world with high population growth and relatively high greenhouse gas emissions, whereas the B2 scenario emphasizes local environmental sustainability, lower population growth, and reduced cumulative emissions [35]. Both scenarios are based on a 1% annual increase in effective CO_2 concentration after 1990 and use the 1961–1990 baseline period.

In this study, the CGCM2 A2 scenario was selected as the primary emissions pathway because it produces stronger climate change signals and has been widely used in Canadian watershed-scale impact studies, facilitating methodological comparison [7,25]. The selection of the CGCM2 A2 scenario follows established practice in Canadian watershed climate impact studies [21,25]. The A2 scenario represents a heterogenous, regionally oriented world with high population growth and relatively high greenhouse gas emissions, providing an upper-bound warming scenario suitable for stress-testing adaptation strategies. Although newer CMIP5/CMIP6 models and Shared Socioeconomic Pathways (SSPs) scenarios offer improved spatial resolution and updated forcing pathways, our focus is on the methodological development and validation of the downscaling framework. Moreover, the broad warming signals (e.g., winter warming, increased summer precipitation variability) derived from CGCM2 A2 are consistent with those reported from CMIP5/CMIP6 ensembles over southern Ontario [26,27], supporting the robustness of the directional changes identified here. A limitation, which we acknowledge, is that a single GCM and scenario cannot capture the full uncertainty envelope; future work should employ multi-model ensembles.

Meanwhile, the B2 scenario is acknowledged as representing a more moderate alternative. The use of a single climate model and emissions pathway introduces uncertainty and does not capture the full range of possible future conditions [36]. Therefore, projected changes should be interpreted as indicative of plausible trends under a high-emissions future rather than precise predictions. The SDSM framework developed here can be extended in future work to multi-model ensembles from CMIP5 or CMIP6 and their associated Shared Socioeconomic Pathways to better quantify uncertainty [37].

3. Methodology and Model Set Up

3.1. Statistical Downscaling Model (SDSM) Procedure and Setup

SDSM downscaling, as outlined by Wilby et al. [23], Gagnon et al. [20], and Harpham and Wilby [38], involves: (a) obtaining historical NCEP predictor data for 1961–2001 (https://www.cpc.ncep.noaa.gov/, accessed on 21 March 2025); (b) selecting key predictors to calibrate regression models (e.g., for P_{mean}, T_{max}, T_{min}) using 1961–1990 baseline data; (c) validating these models against 1991–2001 data; (d) iteratively refining predictors until validation statistics are satisfactory; (e) applying the validated models to downscale future climate variables using CGCM2 predictor data until 2100. SDSM version 4.2 (https://sdsm.org.uk/software.html, accessed on 5 December 2024) facilitates this process through built-in modules for variable screening, model calibration, weather generation, and scenario analysis [16].

Because SDSM downscales to a single point (the Fergus station), we implicitly assume that the station's climate is representative of the entire Canagagigue Creek Watershed. This introduces spatial representativeness uncertainty, especially for precipitation, which can vary locally. However, given the watershed's small area (53 km^2) and low topographic relief, the use of a single station is acceptable for a first-order assessment. Future work could employ multi-site downscaling to better capture spatial heterogeneity. The primary value of statistical downscaling in this study is not to resolve sub-basin spatial heterogeneity (which is limited) but to generate daily time-series data from coarse GCM outputs, preserving temporal variability and extremes at the watershed scale [12,15].

3.1.1. Predictands and Predictors

Daily observed weather variables for Fergus, Ontario (1961–2001), including maximum temperature (T_{max}), minimum temperature (T_{min}), and mean precipitation (P_{mean}), were extracted using Environment Canada's Climate Data Extracting (CDEX) tool [39,40]. These variables served as the local predictands for SDSM calibration and validation. Missing values, flagged as −99 in the Canadian Daily Climate Data (CDCD), were handled directly by SDSM. For trend analysis, missing entries were interpolated using adjacent daily averages. Predictor variables were sourced from the National Centers for Environmental Prediction (NCEP) reanalysis dataset (1961–2001), available via the Canadian Climate Change Scenarios Network (CCCSN). Predictors from 1961–1990 were used to calibrate multiple linear regression models for each predictand. The same predictor types were applied to validate the model over 1991–2001. The 25 NCEP predictors considered for downscaling.

The large-scale atmospheric predictors used for SDSM downscaling, representing surface and upper-air circulation, thermodynamic, and moisture conditions. These include mean sea level pressure (mslp), surface airflow strength (p_f), surface zonal (p_u) and meridional (p_v) wind velocities, surface vorticity (p_z), wind direction (p_th), and divergence (p_zh). Upper-air circulation is characterized at the 500 hPa level by airflow strength (p5_f), zonal (p5_u) and meridional (p5_v) velocities, vorticity (p5_z), geopotential height (p500), wind direction (p5th), and divergence (p5zh). Similarly, conditions at the 850 hPa level are represented by airflow strength (p8_f), zonal (p8_u) and meridional (p8_v) velocities, vorticity (p8_z), geopotential height (p850), wind direction (p8th), and divergence (p8zh). Moisture-related predictors include specific humidity at 500 hPa (s500), at 850 hPa (s850), and at the surface (shum), along with mean air temperature at 2 m (temp).

Following successful validation, the calibrated regression parameters were applied to CGCM2 A2 scenario predictors (2015–2044) to downscale daily weather series. Predictor selection was based on statistical correlation strength and climatological relevance, with transformations applied where necessary to improve model performance. Precipitation downscaling was treated as a conditional process, while temperature was modeled unconditionally. The mathematical formulations used for both processes, including transformation, bias correction, and variance inflation, are detailed in Supplementary Material S2.

3.1.2. Calibration and Validation

SDSM calibration was performed using the 1961–1990 period, while validation employed data from 1991–2001. The model generated monthly parameter files (PAR) containing regression coefficients for each selected predictor and associated statistical diagnostics, including standard error and the linear regression correlation coefficient, r-squared. Monthly calibration allowed for improved seasonal representation. For temperature variables, unconditional linear regressions were applied, while precipitation calibration used a conditional process based on exceedance probability thresholds. The "Weather Generator" module was used to simulate daily climate series during both calibration and validation periods using ensemble sizes of 100 realizations. Validation results were assessed through visual (Quantile–Quantile (Q-Q) and probability density function (PDF) plots) and statistical means. SDSM Summary Statistics show monthly observed/downscaled predictand characteristics (mean, max, min, variance; plus dry/wet spells for precipitation) from daily data.

3.1.3. Performance Evaluation

This Performance of the downscaled climate variables was evaluated using standard model evaluation metrics (equations in Supplementary Material S3), including Nash-Sutcliffe Efficiency (NSE), Root Mean Square Error (RMSE), and the Coefficient of Determination (R^2). These metrics were computed for each variable at monthly time steps. Following Moriasi et al. [41], NSE values greater than 0.5, RMSE values within 70% of the standard deviation of observed data, and R^2 values above 0.5 were considered acceptable (Table S1 in Supplementary S3). Q-Q and PDF plots were also examined to ensure graphical agreement between observed and simulated values. Once calibration results satisfied these thresholds, validation for 1991–2001 was performed using the same predictors, and performance metrics were recalculated to confirm robustness. In addition to conventional performance metrics (NSE, RMSE, and R^2), model performance was evaluated. Across the full distribution of observed and downscaled climate variables involved the use of Q-Q plots, PDF comparisons, and variance diagnostics. These distribution-based analyses

https://doi.org/10.3390/cli14070150

enabled assessment of lower, median, and upper quantiles, including the representation of extreme events and tail behavior.

3.1.4. Uncertainty Analysis and Scenario Generation

To evaluate the statistical consistency between observed and downscaled datasets, non-parametric tests including the Kolmogorov–Smirnov (K-S) two-sample test and the Wilcoxon Signed Rank (W-S) test were conducted at a 95% confidence level. These tests were applied to assess distributional similarity between observed and downscaled datasets across the full range of climatic conditions. They also helped identify potential biases beyond conventional mean-based performance metrics, including differences associated with variability and extreme events. A p-value below 0.05 indicated statistically significant differences. Full mathematical formulations are provided in Supplementary Material S4. Once model performance was validated, the "Scenario Generator" function in SDSM was used to downscale CGCM2 A2 predictors for the 2015–2044 period. An ensemble mean of 100 realizations was generated, and leap years were manually adjusted by interpolating February 29th values from adjacent dates.

3.1.5. Weather Variable Distribution and Trend Analysis

The probability density function (PDF) plots of observed monthly averaged daily weather variables (P_{mean}, T_{max}, T_{min}) at Fergus, Ontario, were compared by decade (1940–2003) to assess distribution changes. After confirming that SDSM-downscaled predictands accurately represented historical local conditions, linear trend analysis was performed for both historical and future periods using monthly averaged daily downscaling results. Historical data (1940–2002) for monthly averages, variances, and precipitation totals were analyzed with MYSTAT 12, applying least squares regression and testing slope significance at the 95% confidence level. Monthly trends of observed and downscale predictands were compared for consistency, and historical downscaled trends were compared to future projections. Positive slopes indicate increasing trends; negative slopes indicate decreasing trends.

Predictand and predictor relationships were established within the Statistical Downscaling Model (SDSM) using correlation analysis and conditional screening to ensure statistical significance ($p < 0.05$) and physical realism. Predictor selection followed an iterative procedure guided by prior studies and sensitivity testing, resulting in physically distinct predictor sets for precipitation and temperature.

Daily precipitation (P_{mean}) was primarily governed by large-scale circulation and moisture conditions. Selected predictors include mean sea-level pressure, which represents synoptic-scale pressure systems, and surface divergence and meridional velocity, capturing low-level convergence and vertical motion. Moisture transport and availability were characterized using 850 hPa zonal and meridional winds and specific humidity at the surface, 850 hPa, and 500 hPa. Geopotential height at 500 hPa was also included to represent mid-tropospheric circulation patterns influencing precipitation development.

In contrast, daily maximum and minimum temperatures (T_{max} and T_{min}) were dominated by thermodynamic controls. Both variables were most strongly correlated with near-surface air temperature at 2 m, surface specific humidity, mean sea-level pressure, and 500 hPa geopotential height. These predictors collectively capture air-mass characteristics, vertical atmospheric structure, and local energy balance processes controlling temperature variability.

The clear physical separation between precipitation and temperature-related predictors supports the robustness of the SDSM setup and enhances confidence in its application for downscaling future climate scenarios.

https://doi.org/10.3390/cli14070150

4. Results

4.1. Calibration and Validation Strategy

Model calibration was conducted for the baseline period from 1961 to 1990, while validation was performed over two independent periods: 1991 to 2001 and 1981 to 2001. The extended validation period (1981 to 2001) was additionally used to assess historical monthly trends and to evaluate the robustness of the calibrated parameter files prior to their application in future climate scenario generation. Calibration performance was first evaluated using Q–Q plots for T_{max}, T_{min}, and P_{mean} (Figure S2 of Supplementary Material S5). For both temperature variables, the Q-Q plots indicate that the majority of downscaled ensemble means closely follow the 1:1 line, suggesting that simulated and observed distributions are statistically consistent across most quantiles.

The Q–Q plots also provide an explicit quantile-based evaluation of model performance across lower, median, and upper quantiles. For temperature variables, the close agreement observed across most quantiles indicates that SDSM reliably reproduces not only the central tendency but also the distributional behavior associated with low- and high-end temperature extremes. In contrast, the increasing divergence observed in the upper precipitation quantiles indicates greater uncertainty in simulating heavy rainfall events, reflecting the known challenges of statistically downscaling intermittent and convective precipitation processes (Figure S2).

Further evidence of the accuracy of temperature downscaling is provided by the PDF plots shown in Figure 2. These figures demonstrate strong agreement between observed and downscaled distributions of daily T_{max} and T_{min} during the calibration period, with similar central tendencies and comparable variability. Minor deviations are confined to the distribution tails; however, overall agreement confirms that SDSM effectively reproduces both the mean state and variability of temperature. Together, the Q-Q and PDF analyses indicate high fidelity in the statistical representation of temperature processes.

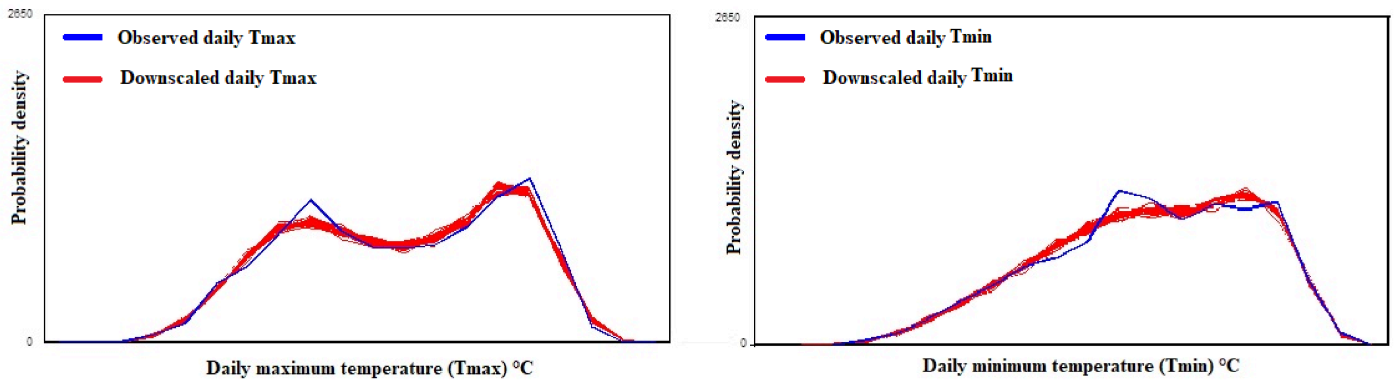

Figure 2. PDF plot of observed and downscaled daily T_{max} and T_{min} for 1961–1990.

In contrast, precipitation calibration results reveal substantially greater uncertainty. The Q-Q plot for P_{mean} (Supplementary Figure S2) shows increasing divergence at higher quantiles, with the model tending to underestimate light rainfall events (0–16 mm) and overestimate heavier precipitation amounts (16–35 mm). This behavior reflects a well-documented limitation of statistical downscaling approaches, which struggle to capture the non-linear, localized, and convective nature of precipitation processes. The increasing ensemble spread with rainfall magnitude further highlights elevated uncertainty in simulating extreme precipitation events.

Validation over the period 1991–2001 confirms these contrasting performance characteristics (Figure 3). Statistical evaluation metrics show excellent performance for temperature variables, with Nash–Sutcliffe Efficiency (NSE) and Coefficient of Determination

(R^2) values exceeding 0.98 at both annual and monthly time scales (Figure 3). These results indicate strong agreement between observed and simulated temperature series and demonstrate the robustness of the calibrated parameter files. In contrast, precipitation validation yields a yearly NSE of 0.71 but a substantially lower monthly NSE of 0.25, highlighting the difficulty of reproducing monthly precipitation variability despite reasonable agreement at the annual scale.

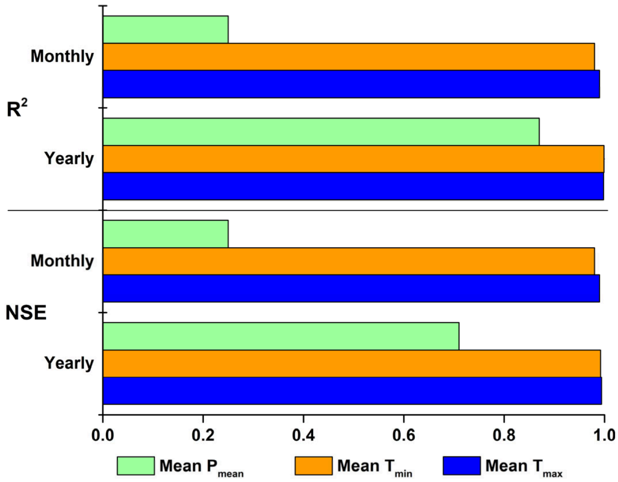

Figure 3. Statistic evaluation of SDSM validation for predictands (1991–2001).

Graphical validation further illustrates these patterns. Figure 4 compares observed and downscaled monthly statistics of T_{max} averaged over 1991–2001. The model accurately reproduces monthly mean T_{max} in most months, with minor discrepancies observed in February and March. Simulated maximum T_{max} values are slightly higher than observations from April through September, while simulated minimum values are marginally higher in March, April, October, and November. Variance is modestly overestimated during warmer months and underestimated during winter, indicating some seasonal bias in temperature variability. Despite these differences, overall agreement remains strong, consistent with the high NSE and R^2 values.

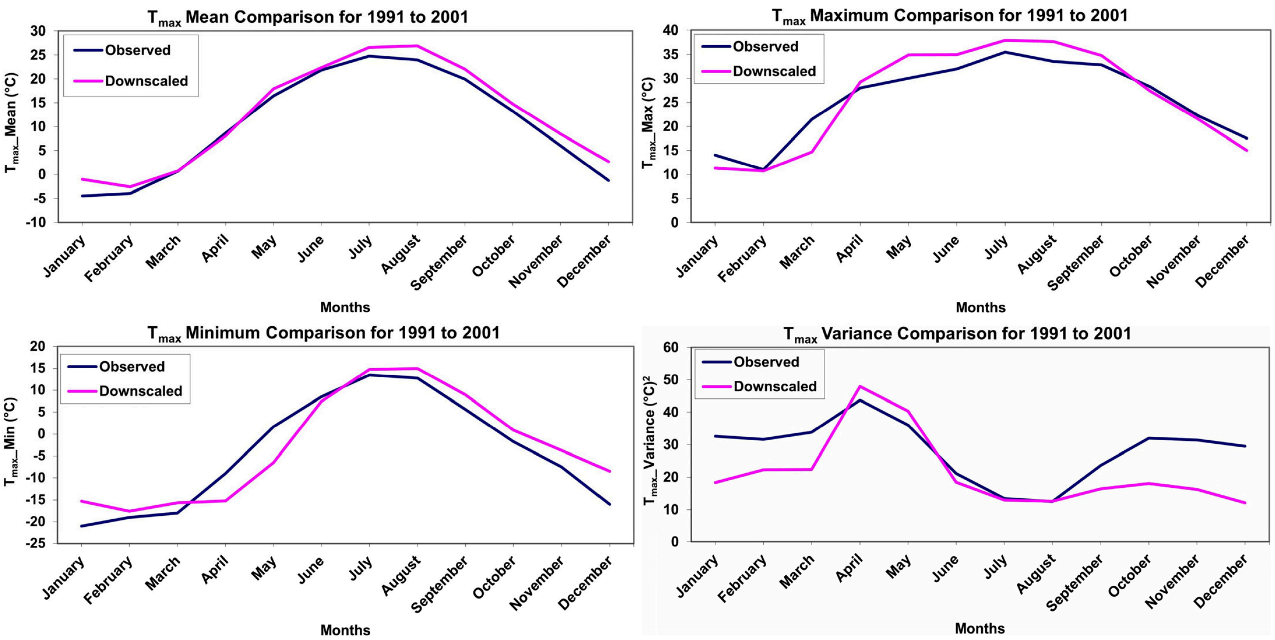

Figure 4. Validation of observed and downscaled T_{max} (°C).

Similarly, Figure 5 presents the validation results for T_{min}. Simulated monthly means are slightly higher than observed values during winter months but lower during late spring and early summer. Maximum T_{min} is overestimated in January, July, and September and underestimated in March, while variance is notably overestimated in March and April. These discrepancies likely reflect transitional seasonal dynamics; nevertheless, the overall performance remains strong, indicating that SDSM reliably captures T_{min} variability at monthly and seasonal scales.

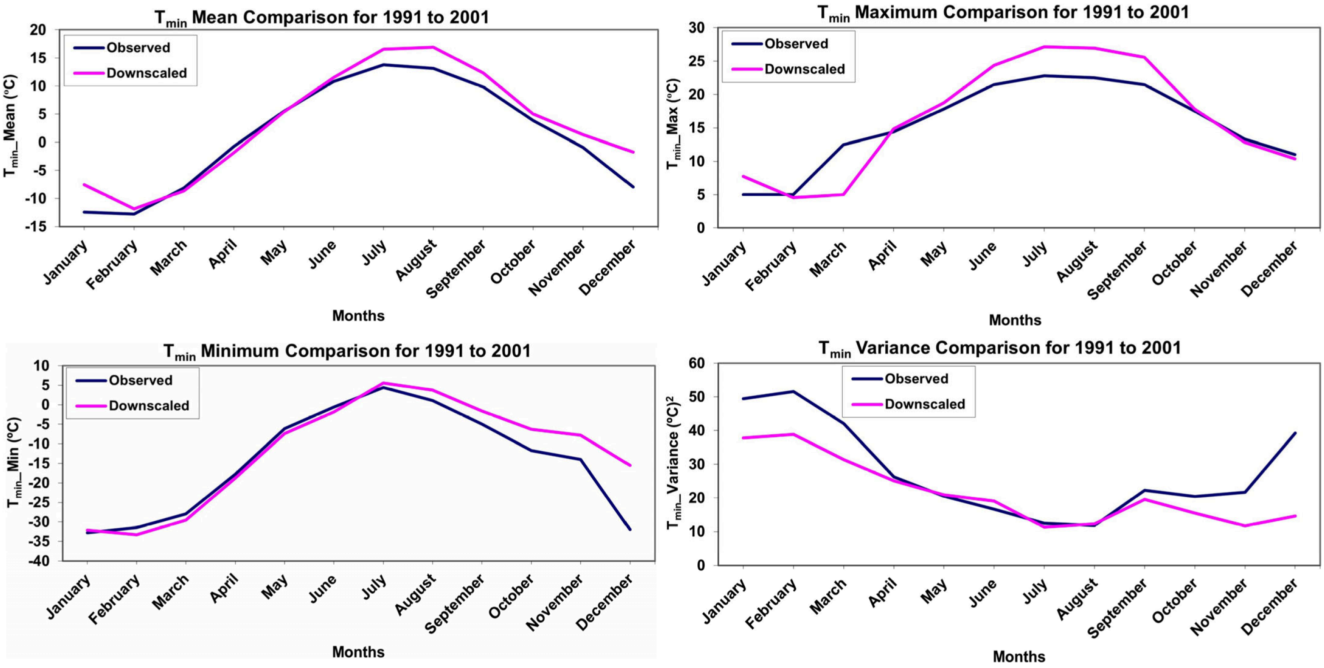

Figure 5. Validation of observed and downscaled T_{min} (°C).

Precipitation validation results, shown in Figure 6, reveal substantially weaker agreement. The simulated mean P_{mean} exceeds observations only in May and September. Variance is considerably overestimated in May, July, and September and underestimated in June and August. In addition, the model consistently underestimates both dry and wet spell lengths, indicating difficulty in reproducing precipitation persistence and event sequencing. These deficiencies underscore the inherent challenges in statistically downscaling precipitation, particularly during warm months dominated by convective processes.

The extended validation period (1981–2001) provides further insight into calibration versus validation performance (Table 2). Monthly evaluation metrics for T_{max} indicate generally strong performance, with most months exhibiting NSE values above 0.6 and R^2 values exceeding 0.7. March stands out as a notable exception, with an NSE close to zero and reduced R^2, indicating poor predictive skill during this transitional month. September also shows elevated errors, reflected by higher RMSE values. T_{min} results follow a similar pattern, with acceptable performance across most months but increased errors in March and September, suggesting heightened uncertainty during seasonal transitions.

Precipitation performance during the extended validation period is markedly weaker. NSE values are below 0.2 for most warm-season months, with August exhibiting a negative NSE and an R^2 of zero, indicating statistically unacceptable performance. More satisfactory results are confined to colder months such as March, October, and December. This pronounced seasonal dependence suggests that SDSM performs better for precipitation driven by large-scale synoptic systems than for high-intensity warm-season rainfall events. These findings are consistent with the calibration Q-Q analysis and confirm that precipitation downscaling uncertainty is both magnitude- and season-dependent. The relatively poor performance for precipitation, particularly in warm months, is not caused by the CGCM2 scenarios but is a well-recognized limitation of statistical downscaling methods like SDSM. Precipitation processes are non-linear, intermittent, and strongly influenced by local convection, which linear regression models cannot fully capture. This is consistent with numerous SDSM applications worldwide (e.g., Wilby et al. [12]).

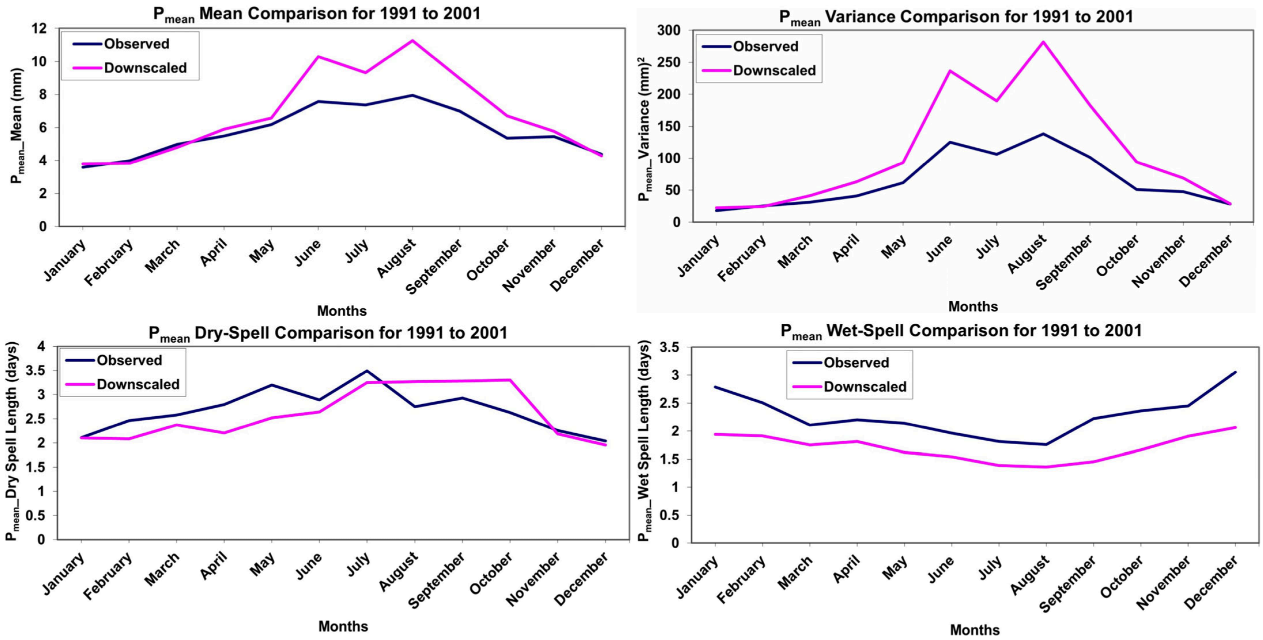

Figure 6. Validation of observed and downscaled P_{mean} (mm).

Table 2. Statistical evaluation summary for T_{max}, T_{min} and P_{mean} downscaling (1981 to 2001).

Parameters	Statistics	Jan	Feb	Mar	Apr	May	Jun	Jul	Aug	Sep	Oct	Nov	Dec
T_{max}	NSE	0.78	0.61	0.03	0.70	0.87	0.65	0.79	0.75	0.36	0.84	0.58	0.85
	RMSE	1.10	1.41	1.89	1.04	0.86	0.87	0.69	0.71	1.10	0.65	1.16	1.06
	R^2	0.80	0.67	0.43	0.76	0.92	0.70	0.82	0.82	0.57	0.84	0.63	0.93
T_{min}	NSE	0.66	0.54	0.22	0.49	0.77	0.60	0.53	0.65	0.39	0.55	0.75	0.83
	RMSE	1.92	1.94	1.91	1.07	0.96	0.80	0.71	0.70	0.89	0.84	0.76	1.25
	R^2	0.73	0.78	0.51	0.70	0.95	0.90	0.64	0.80	0.67	0.71	0.76	0.94
P_{mean}	NSE	0.20	0.24	0.46	0.33	0.11	0.16	0.08	−0.08	0.15	0.52	0.32	0.46
	RMSE	0.71	0.93	0.56	0.84	0.97	1.27	1.26	1.66	1.71	0.71	1.00	0.69
	R^2	0.45	0.37	0.53	0.49	0.22	0.19	0.17	0.00	0.15	0.56	0.38	0.55

Overall, the comparison between calibration and validation periods demonstrates that SDSM provides highly reliable downscaling of T_{max} and T_{min}, with consistent performance across multiple time scales and validation windows. In contrast, precipitation downscaling remains challenging, particularly for warm months and extreme events. While annual precipitation totals are reasonably captured, monthly variability, variance, and spell characteristics are less well-reproduced. These limitations necessitate cautious interpretation of future precipitation projections and justify the inclusion of uncertainty analyses when applying the calibrated parameter files to CGCM2 climate scenario simulations. A limitation of this validation is the absence of the most recent two decades (2005–2025) due to data availability at the time of the study. However, the validation period 1991–2001 already includes warmer conditions compared to the calibration baseline, and the model's good performance during that period provides reasonable confidence.

4.2. Uncertainty Analysis

To supplement the statistical evaluation, non-parametric tests were used to analyze uncertainty in the downscaled data for the period 1981–2001. The Kolmogorov–Smirnov (K-S) test assessed whether observed and downscaled data came from the same distribution, while the Wilcoxon Signed Ranks (W-S) test evaluated if their means were significantly different.

The K-S test (Table 3) showed that for T_{max}, no monthly p-values were below 0.05, indicating no significant difference in distributions. For T_{min}, significant differences were found in June and September. P_{mean} showed significant differences in February, April, and July, reinforcing its higher uncertainty.

Table 3. p-values of K-S test for observations and downscaled predictands (1981–2001).

Predictands	Jan	Feb	Mar	Apr	May	Jun	Jul	Aug	Sep	Oct	Nov	Dec
T_{max}	0.546	0.546	0.546	0.172	0.797	0.546	0.797	0.323	0.172	0.969	0.969	0.546
T_{min}	0.546	0.172	0.172	0.323	0.172	0.013	0.546	0.323	0.035	0.082	0.797	0.172
P_{mean}	0.082	0.035	0.172	0.013	0.172	0.172	0.035	0.082	0.172	0.797	0.323	0.082

The W-S test (Table 4) indicated significant shifts in the means of T_{max} (Feb, Dec) and T_{min} (Jan, Feb, Apr–Aug, Dec) between the downscaled and observed data. These shifts were consistent with an actual observed warming trend between the calibration baseline (1961–1990) and the validation period (1981–2001), as confirmed by box plot analysis (see Supplementary Material S6). No significant mean shifts were detected for P_{mean}.

Table 4. p-values of W-S test for observed and downscaled predictands (1981 to 2001).

Predictands	Jan	Feb	Mar	Apr	May	Jun	Jul	Aug	Sep	Oct	Nov	Dec
T_{max}	0.546	0.546	0.546	0.172	0.797	0.546	0.797	0.323	0.172	0.969	0.969	0.546
T_{min}	0.546	0.172	0.172	0.323	0.172	0.013	0.546	0.323	0.035	0.082	0.797	0.172
P_{mean}	0.082	0.035	0.172	0.013	0.172	0.172	0.035	0.082	0.172	0.797	0.323	0.082

Overall, the uncertainty analysis confirmed that the SDSM parameters for T_{max} and T_{min} were robust and suitable for generating future scenarios. The parameters for P_{mean}, while less accurate, were deemed acceptable for use in scenario generation given the inherent challenges of precipitation downscaling.

4.3. GCM Scenario Generation

The calibrated SDSM was applied to generate daily future climate scenarios for a 30-year period (2015–2044) using the established regression relationships with CGCM2 A2 scenario predictors. The downscaled projections were then systematically compared with a historical 30-year baseline period (1961–1990), derived from observed NCEP predictors, to quantify projected changes in temperature and precipitation patterns.

The use of consistent 30-year periods for both the baseline and projection horizons is essential to ensure statistical reliability in model calibration and validation. A 30-year timeframe reduces the influence of short-term variability and interannual fluctuations, allowing for a stable comparison between observed and projected datasets. This approach strengthens the robustness of the calibration process and improves the consistency and credibility of the downscaled climate projections.

Figure 7 summarizes projected changes in monthly T_{max} by integrating mean, maximum, minimum, and variance statistics. The results indicate clear seasonal contrasts. Winter months (December to March) exhibit higher mean and minimum T_{max}, accompanied by reduced variance, indicating warmer and more thermally stable winters. Fall months show a similar pattern of increased mean and minimum T_{max} with decreased variability. In contrast, summer warming is characterized by increases in mean, maximum, and minimum T_{max}, particularly in July and August, while variance remains relatively unchanged. Spring months display only minor changes, suggesting limited sensitivity during the seasonal transition. Overall, T_{max} downscaled projections point to warmer winters and hotter summers, with reduced cold-season variability.

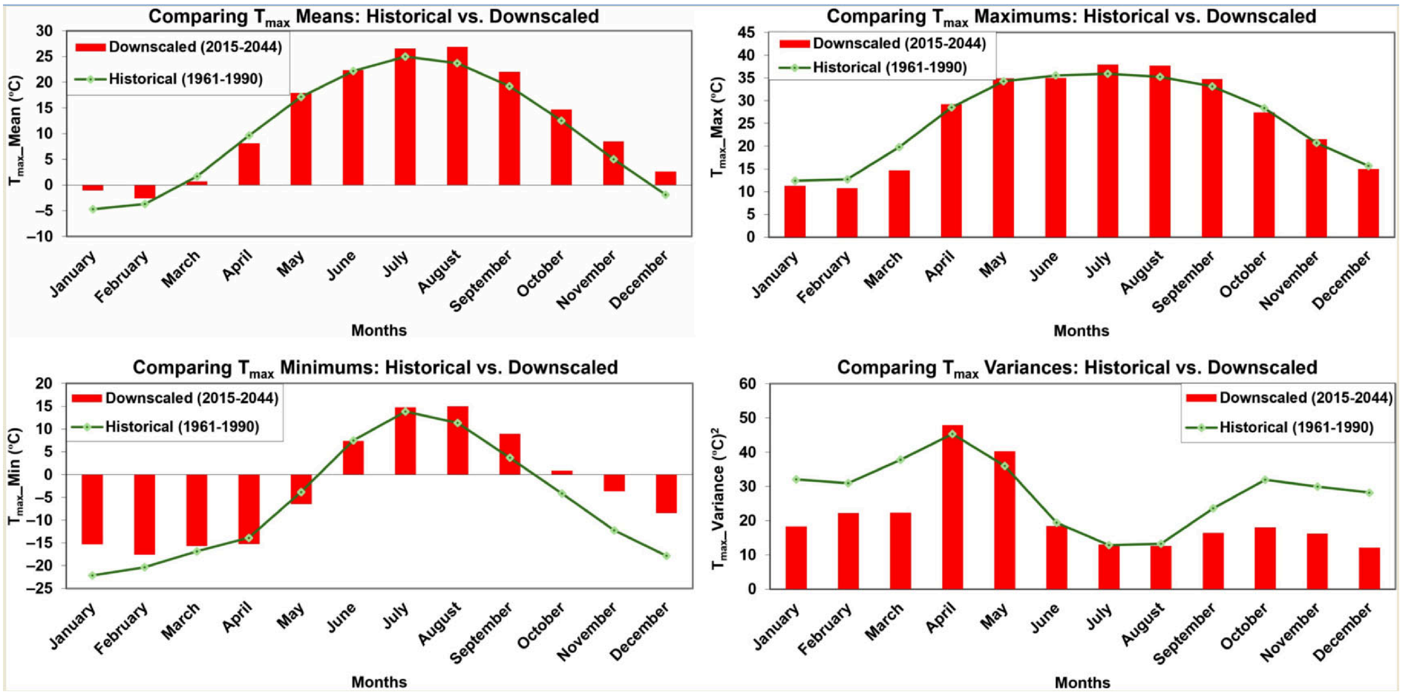

Figure 7. Comparison of historical (1961–1990) and downscaled (2015–2044) monthly T_{max} (mean, max, min, variance).

Changes in T_{min} are more pronounced and consistent, as shown in Figure 8, which combines mean, maximum, minimum, and variance statistics. Mean T_{min} increases substantially during winter and from mid-summer through late fall, while minimum T_{min} shows especially large increases in December and late summer–fall months. Variance in T_{min} decreases across most months, particularly during cold seasons, indicating a strong reduction in cold extremes and enhanced nighttime warming. Summer months also experience notable increases in mean and maximum T_{min}, implying warmer nights and elevated heat stress. Compared to T_{max}, T_{min} exhibits stronger warming signals and greater seasonal coherence, reinforcing its sensitivity to greenhouse forcing.

Downscaled projected precipitation changes, summarized in Figure 9, reveal modest shifts in monthly means but substantial changes in extremes and variability. Mean P_{mean} increases slightly during summer and early fall, while maximum precipitation shows large increases in warm months, particularly June and August. Variance increases sharply during summer and early fall, indicating heightened precipitation variability. Dry spell lengths are projected to increase in late summer and fall, suggesting longer intervals without rainfall, while wet spell lengths shorten across most months, indicating more intermittent precipitation. Projected increases in precipitation variance, together with shortened wet-spell duration and increased upper-tail spread, suggest an increasing likelihood of short-duration, high-intensity rainfall events despite relatively stable monthly mean precipitation. This combination suggests that future precipitation may occur in more intense, short-duration events interspersed with longer dry periods.

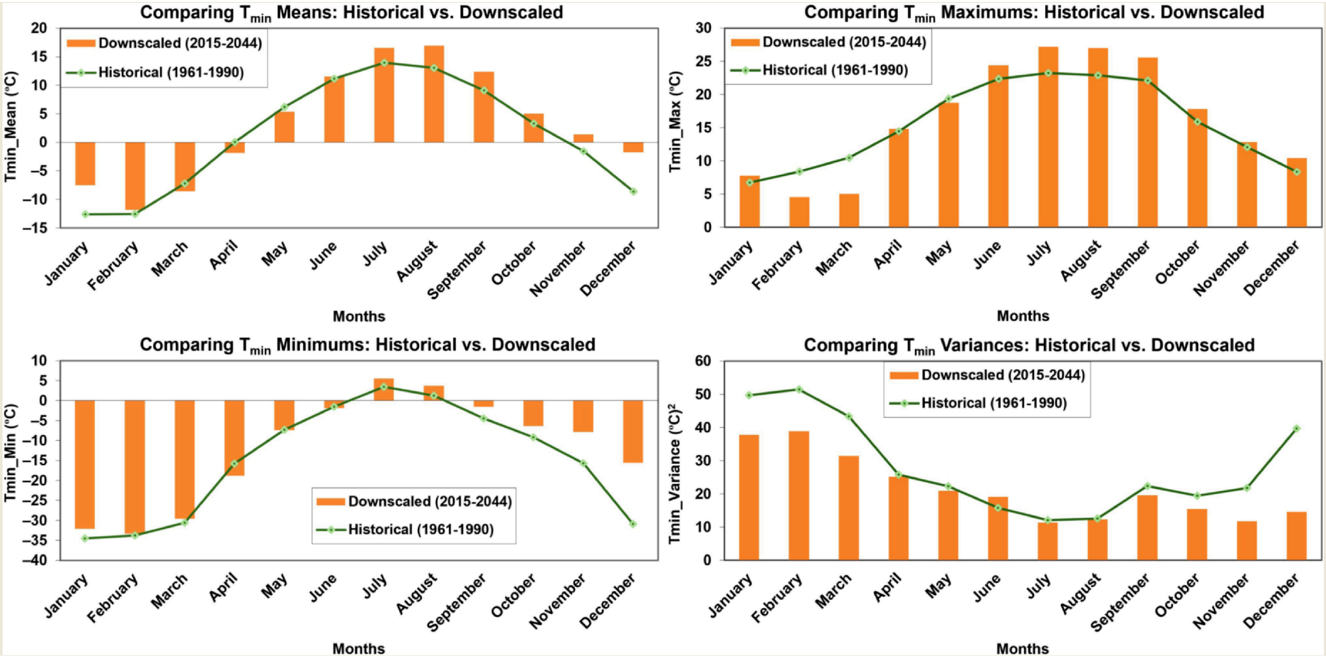

Figure 8. Comparison of historical (1961–1990) and downscaled (2015–2044) monthly T_{min} (mean, max, min, variance).

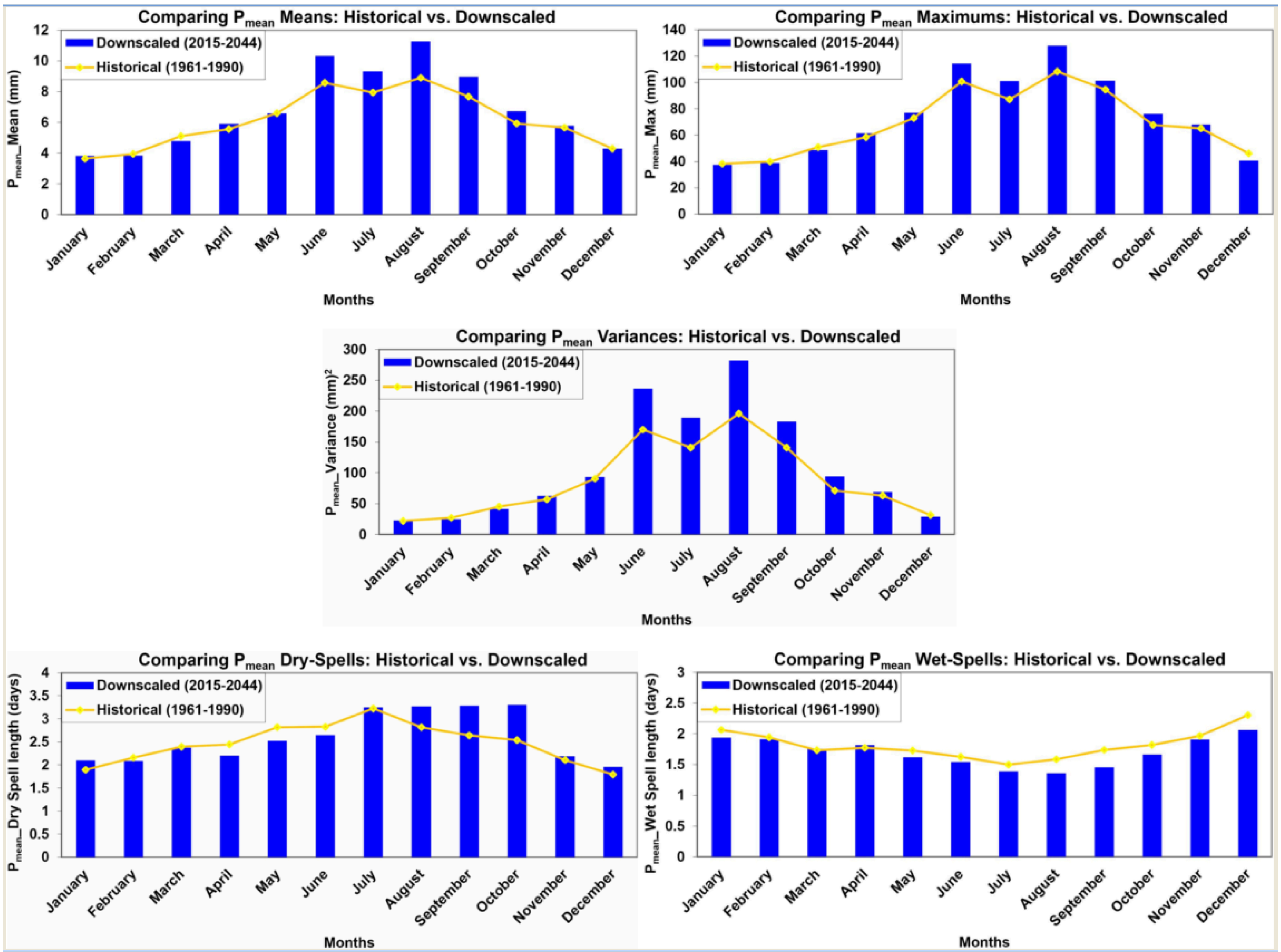

Figure 9. Comparison of historical (1961–1990) and downscaled (2015–2044) monthly P_{mean} (max, variance, dry- and wet-spell lengths).

In summary, the combined analysis indicates a future climate characterized by strong warming, especially in T_{min}, reduced cold-season temperature variability, and increasingly variable and episodic precipitation. While mean precipitation changes remain modest, the projected increase in rainfall intensity and summer variability highlights heightened risks of flooding, erosion, and late-season drought. These results emphasize the importance of considering variability and extremes, rather than means alone, when assessing future climate impacts at the watershed scale.

4.4. Historical Climate Trends (1940–2003)

To assess existing climatic trends and evaluate the consistency of future climate projections, a historical trend analysis was conducted comprising two components: probability distribution analysis and linear trend analysis of key weather variables.

The probability density function (PDF) plots of monthly mean maximum temperature (T_{max}), minimum temperature (T_{min}), and precipitation (P_{mean}) were developed for six decadal intervals spanning 1940–2003. Figure 10 illustrates the decadal PDFs of T_{max}, categorized at 5 °C intervals between −25 °C and 30 °C. The general shapes of the PDFs are consistent across decades; however, a clear rightward shift is observed in later decades, particularly during 1990–2003, with increased probabilities associated with T_{max} values above 0 °C. This shift provides evidence of a gradual warming trend, especially during winter months, with fewer extreme cold events.

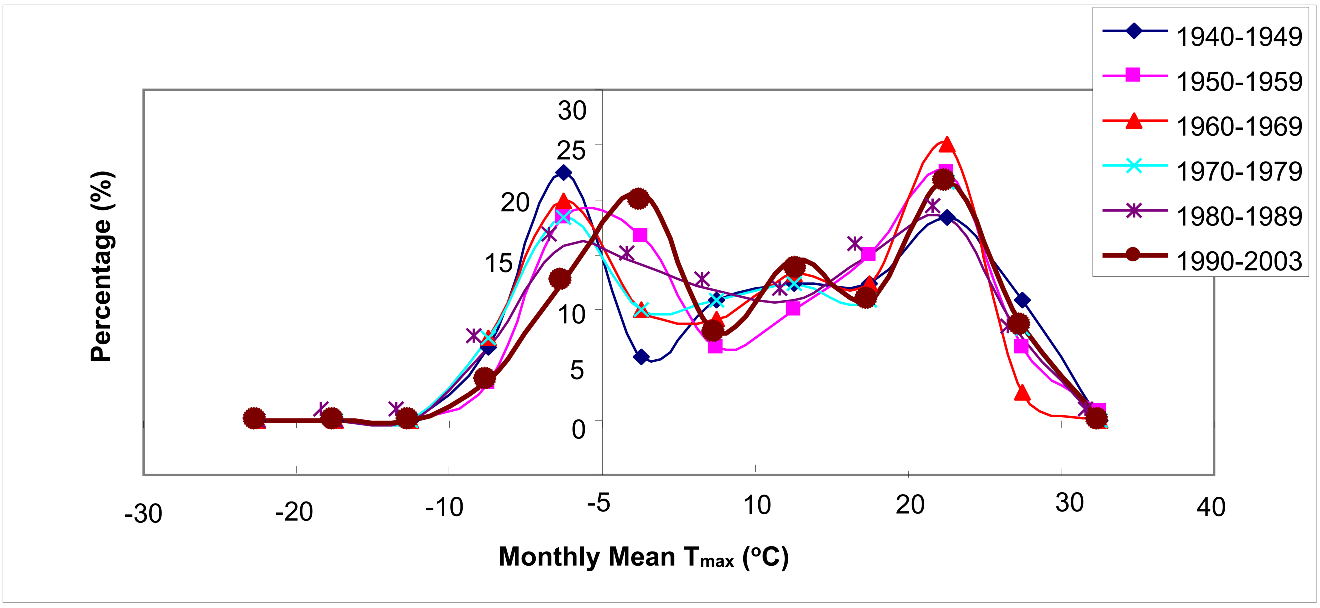

Figure 10. PDF plots of monthly mean T_{max} per decade from 1940 to 2003.

The T_{min} distributions, presented in Figure 11, exhibit a similar pattern. While the overall shapes remain stable, the left tail of the distribution (temperatures below 0 °C) shifts upward across decades, indicating a reduction in extremely low T_{min} values, particularly in the most recent decade. Unlike T_{max}, changes on the warmer side of the distribution are less pronounced, suggesting that warming is most evident through milder winter minima rather than through more frequent high values.

Precipitation PDFs, binned at 0.5 mm intervals from 0 to 9 mm (Figure 12), show greater variability. While distributional shapes are broadly consistent across decades, the period 1990–2003 is characterized by a peak occurrence probability at lower precipitation levels compared to previous decades. Additionally, a secondary peak emerges around 3 mm, indicating a potential increase in the frequency of moderate events. This dual-peaked structure suggests greater heterogeneity in rainfall intensity, with more frequent light precipitation punctuated by moderate rainfall events.

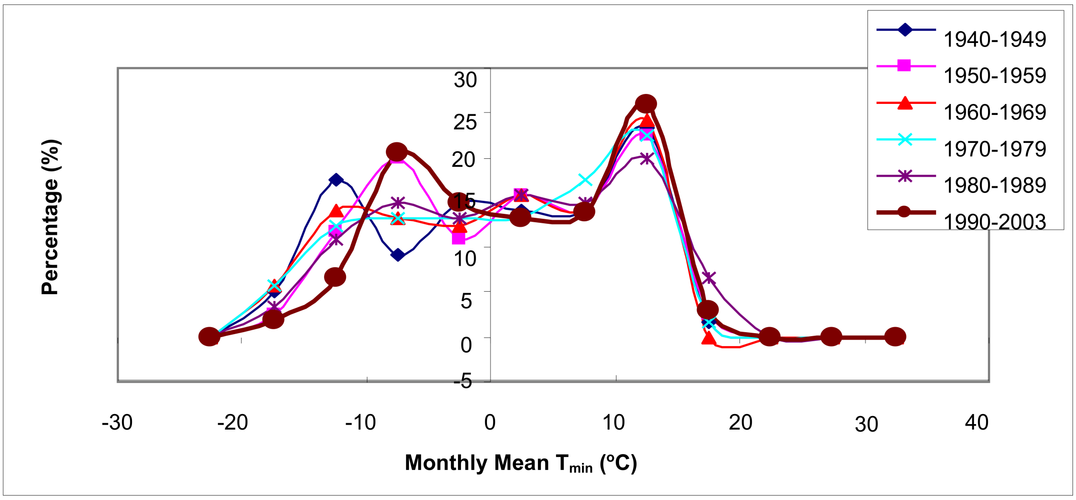

Figure 11. PDF plots of monthly mean T_{min} per decade from 1940 to 2003.

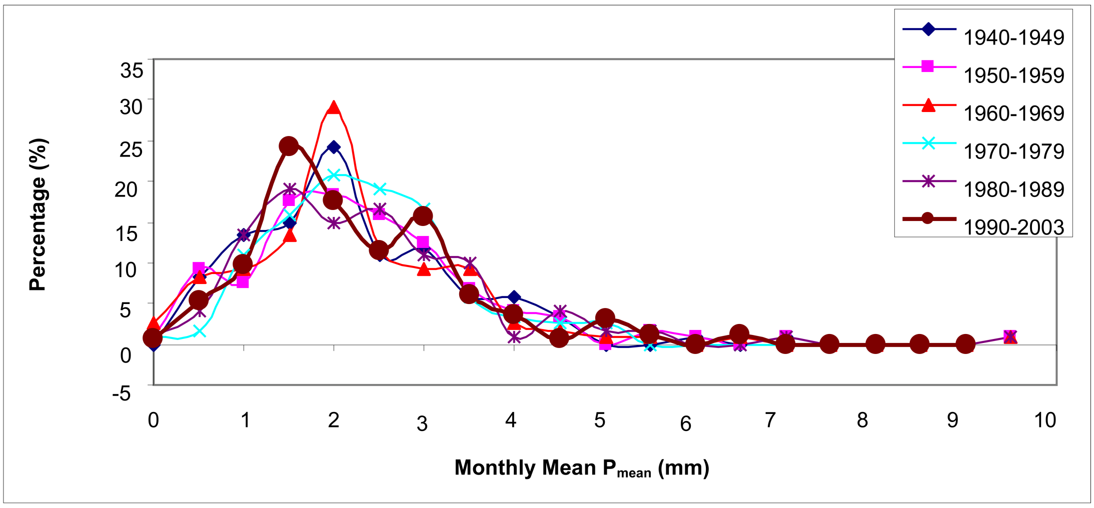

Figure 12. PDF plots of monthly mean P_{mean} per decade from 1940 to 2003.

Overall, these distributional assessments support the assumption that the fundamental probability structures of T_{max}, T_{min}, and P_{mean} have remained stable, justifying the use of linear regression for trend detection. Least squares regression was applied to monthly and annual records of temperature and precipitation for the period 1940–2003.

Linear trend analysis of the observed records from 1940 to 2003 was performed using least squares regression (Supplementary Material S7). The slopes and their associated p-values for a test of a non-zero slope are summarized in Table 5. The results indicate slight positive slopes for monthly total precipitation, yearly total precipitation, monthly mean P_{mean}, and monthly mean T_{max}, though none were statistically significant ($p > 0.05$). Conversely, the variances of monthly mean precipitation, T_{max}, and T_{min} showed slight decreasing trends, while also lacking statistical significance. The monthly mean T_{min} was the only variable exhibiting a potential significant increasing trend ($p = 0.076$).

To further explore monthly-scale patterns, trends for 1982–2000 were examined using both observed and SDSM-downscaled predictands. A three-point moving average was applied to reduce variability. Results are summarized in Table 6, with detailed plots provided in Supplementary Material S8.

Table 5. Results of trend line slope non-zero test.

Statistic	Monthly Total P_{mean}	Yearly Total P_{mean}	Monthly Mean P_{mean}	Monthly Variance of P_{mean}	Monthly Mean T_{max}	Monthly Variance of T_{max}	Monthly Mean T_{min}	Monthly Variance of T_{min}
Slope	0.035	0.420	0.002	−0.054	0.009	−0.015	0.033	−0.025
p-value	0.635	0.632	0.444	0.564	0.656	0.559	0.076	0.391
Conclusion	N.S.	N.S.	N.S.	N.S.	N.S.	N.S.	P. S.	N.S.

N.S. = No Significant evidence in changing trends; P.S. = Possible Significant evidence in change trend.

Table 6. Summary of monthly trend analysis (slope and *p*-value) for observed and SDSM-downscaled T_{max}, T_{min}, and P_{mean}, 1982–2000. (Note: colored value indicates the level of significance).

Variable	Data Set	Items	Jan	Feb	Mar	Apr	May	Jun	Jul	Aug	Sep	Oct	Nov	Dec
T_{max}	Observed	slope	0.130	0.111	0.101	0.000	0.052	0.084	−0.047	0.041	0.086	0.066	0.036	0.088
	Downscaled	slope	0.051	−0.029	−0.064	−0.023	0.023	0.069	−0.064	0.019	−0.036	0.026	−0.013	0.029
	Observed	*p*-value	0.016	0.099	0.006	0.997	0.360	0.000	0.208	0.036	0.006	0.078	0.370	0.047
	Downscaled	*p*-value	0.223	0.505	0.071	0.568	0.607	0.001	0.012	0.172	0.084	0.532	0.746	0.420
T_{min}	Observed	slope	0.081	0.020	0.029	−0.063	0.006	0.107	−0.052	−0.021	−0.023	0.002	−0.010	0.053
	Downscaled	slope	−0.001	−0.042	−0.064	−0.056	0.000	0.075	−0.051	0.014	−0.021	0.007	−0.002	0.042
	Observed	*p*-value	0.247	0.840	0.568	0.183	0.903	0.001	0.071	0.332	0.510	0.960	0.797	0.348
	Downscaled	*p*-value	0.982	0.406	0.021	0.075	0.993	0.000	0.005	0.336	0.243	0.745	0.941	0.303
P_{mean}	Observed	slope	0.093	−0.015	−0.033	0.004	−0.005	0.068	−0.001	−0.107	−0.087	−0.042	−0.049	−0.046
	Dowscaled	slope	0.017	0.004	−0.028	0.014	−0.018	0.078	0.013	0.000	−0.005	−0.015	−0.045	−0.031
	Observed	*p*-value	0.000	0.528	0.058	0.893	0.783	0.006	0.975	0.002	0.056	0.090	0.039	0.082
	Dowscaled	*p*-value	0.014	0.663	0.004	0.365	0.199	0.003	0.528	0.987	0.650	0.305	0.002	0.002

The downscaled T_{max} data showed more months with decreasing trends than the observed data (Table 6). For instance, downscaled T_{max} indicated negative slopes in February, March, April, September, and November, whereas the observed T_{max} showed positive slopes in these months, significantly so in March and September. The significant increasing trend in June was well-captured by the downscaling. The only observed decreasing trend in July was also captured but with a higher level of significance in the downscaled data.

For T_{min} (Table 6), the only observed significant positive trend was in June ($p = 0.001$), which was accurately replicated by the downscaled data ($p = 0.000$). The downscaled data also indicated a significant negative trend in July ($p = 0.005$), which was present but less significant in the observations ($p = 0.071$). Observed decreasing trends in April, September, and November were captured with higher significance in the downscaled results. Discrepancies were noted in January, February, and March, where observed increases contrasted with downscaled decreases, the latter being significant for March ($p = 0.021$).

Analysis of P_{mean} (Table 6) showed that observed decreasing trends in January, March, April, May, and September through December were generally captured by the downscaled data, often with higher significance. The trends in February were not significant for either dataset. The reliability of the downscaled trend results for July and August is questionable due to poor SDSM performance metrics (NSE = 0.08 and −0.08, respectively; see Table 2).

In summary, the only climate variable showing a potentially significant historical increasing trend was the monthly mean T_{min}. No significant decreasing trends ($p < 0.01$) were found for observed T_{max} or T_{min}, suggesting a low probability of future cooling. The most consistent significant trend across both observed and downscaled data was an increase in all three variables during June. While some discrepancies existed, all significant trends ($p < 0.01$) in the downscaled predictands reflected trends present in the observed data (e.g., increasing June T_{max} and T_{min}; decreasing March, November, and December P_{mean}). The presence of more numerous and sometimes more significant decreasing trends in the downscaled data compared to the observations may reflect a compromise inherent in the SDSM methodology when applied to the warming-enforced CGCM2 A2 scenario.

4.5. Predicted Climate Projections (2025–2044)

Monthly linear trend analyses were conducted for the downscaled future weather predictands: daily maximum temperature (T_{max}), daily minimum temperature (T_{min}), and daily mean precipitation (P_{mean}), for the period 2025–2044. The analysis primarily focuses on projections derived from the CGCM2 A2 emissions scenario, which is used throughout this study to represent future climate conditions. Monthly trend line plots are presented in Figures 13–15, showing the corresponding trend slopes for the period 2025–2044. The statistical significance levels are summarized in Tables S2.1–S2.3 in Supplementary Material (S9).

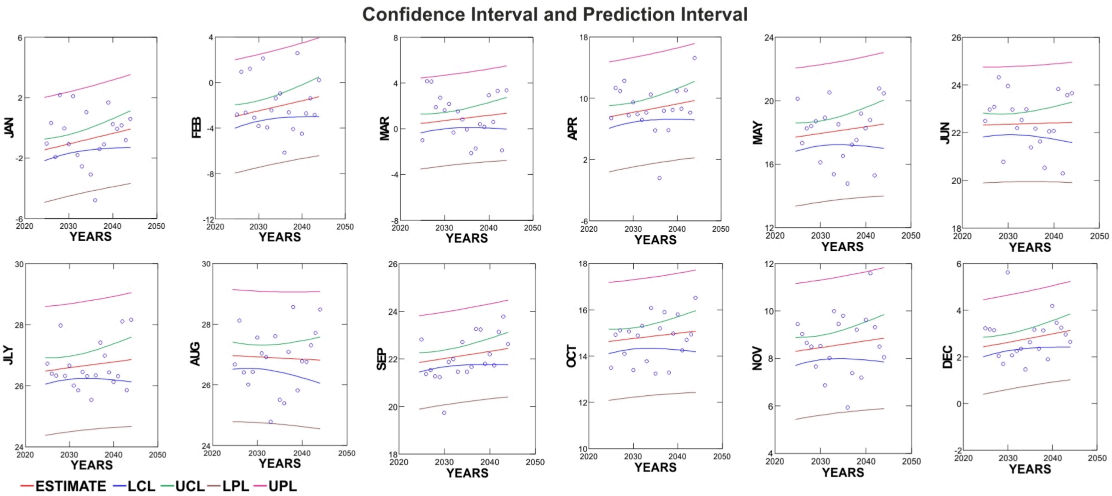

Figure 13. Monthly trend plots of SDSM-downscaled T_{max} for 2025 to 2044.

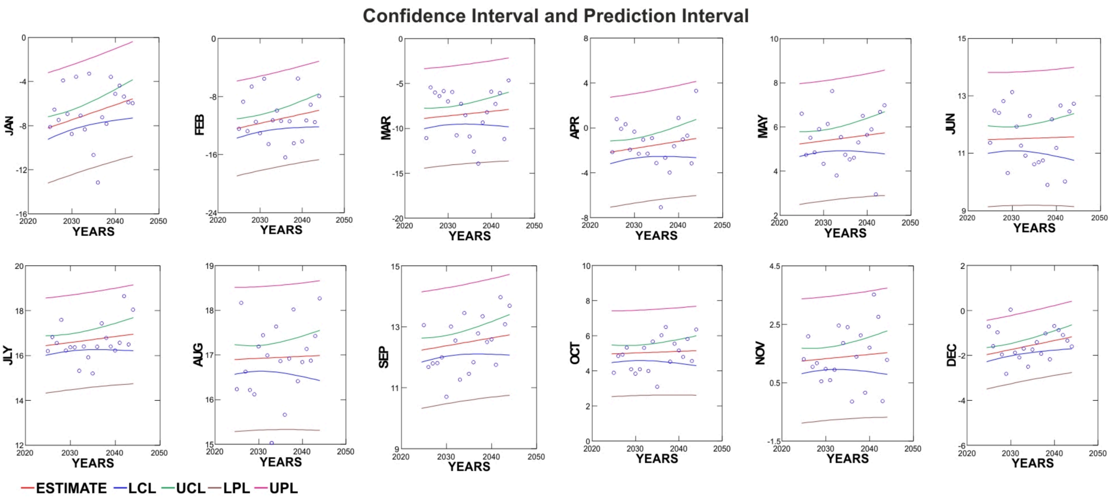

Figure 14. Monthly trend plots of SDSM-downscaled T_{min} for 2025 to 2044.

Projected changes in air temperature reveal a clear warming signal with pronounced seasonal contrasts. For Tmax (Figure 13), positive trends dominate most months, with statistically significant increases ($p < 0.1$) identified in January, February, and December (Table S2.1). These results indicate robust winter warming, consistent with enhanced cold-season sensitivity to greenhouse forcing. Although summer months such as July and August also exhibit increasing T_{max}, the associated trends are weaker and not statistically significant, suggesting that summer warming manifests more through elevated extremes rather than consistent long-term trends. August is the only month showing a negative slope; however, the high p-value (0.730) confirms that this apparent decrease is not statistically meaningful. June exhibits an almost negligible trend, reflecting relative stability in early summer T_{max}.

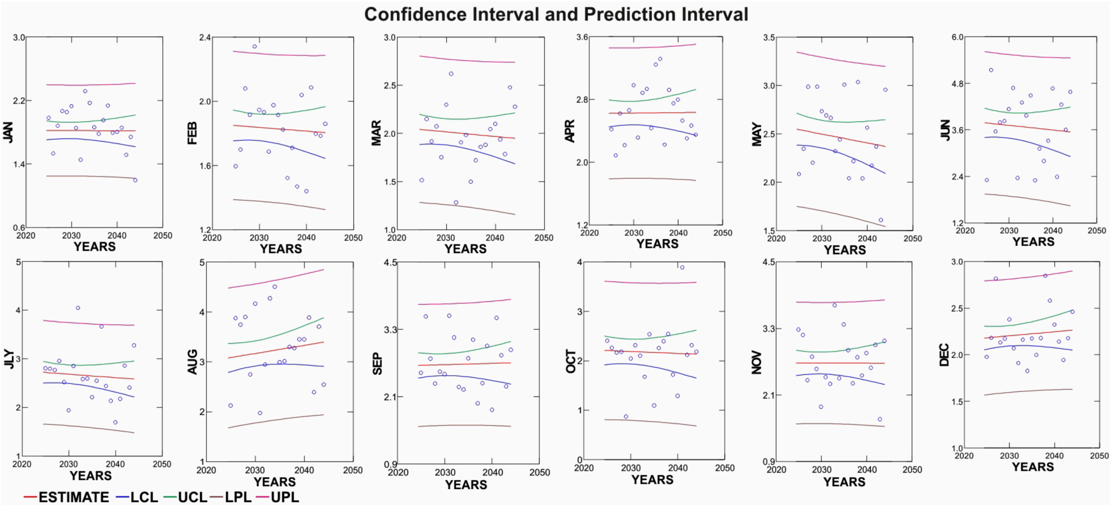

Figure 15. Monthly trend plots of SDSM-downscaled P_{mean} for 2025 to 2044.

Warming trends are more pronounced and statistically robust for T_{min} (Figure 14). Winter months again show the strongest signals, with January and December exhibiting statistically significant positive trends ($p < 0.05$), and February displaying a marginally significant increase ($p < 0.1$) (Table S2.2). No months show decreasing T_{min} trends, indicating a consistent shift toward warmer nighttime and winter conditions. Compared with historical downscaled T_{min}, future projections indicate fewer cooling tendencies and a persistent increase in cold-season minimum temperatures. These changes imply a substantial reduction in extreme cold events and a narrowing of the diurnal and seasonal temperature range, particularly under the higher-emission A2 scenario. Furthermore, earlier analyses of temperature variability (Figures 7 and 8) indicate that both T_{max} and T_{min} variances decrease during winter and fall, reinforcing the projection of more thermally stable cold seasons.

In contrast to temperature, future monthly averaged daily precipitation does not exhibit statistically significant linear trends in any month (Figure 15), as all *p*-values exceed 0.1 and slope magnitudes remain small (Table S2.3). At face value, this suggests negligible long-term change in mean monthly precipitation. However, examination of seasonal patterns and variability reveals important hydrologic implications that are not captured by mean trends alone. Earlier results (Figure 9) demonstrate modest increases in summer and early fall precipitation means, particularly during June, while other seasons show little change or slight decreases.

More importantly, precipitation variability is projected to increase substantially during summer months, as evidenced by higher variances and altered distribution characteristics. Combined with the observed shortening of wet spell lengths and lengthening of dry spells in late summer and early fall (Figure 9), these results strongly suggest an increased likelihood of heavy rainfall events occurring over shorter durations. Thus, despite stable monthly mean precipitation, future rainfall is expected to be delivered in more intense and episodic events, heightening the risk of flooding, erosion, and hydrologic extremes.

Overall, the downscaled future projected climate projections for 2025–2044 indicate a transition toward enhanced winter and summer warming, particularly driven by statistically significant increases in T_{min} during cold months, reduced temperature variability in winter, stable but seasonally redistributed precipitation, and increased indicators of rainfall intensity.

5. Discussion

The results of this study reveal a clear warming signal in the Canagagigue Creek Watershed, driven primarily by statistically significant increases in minimum temperature (T_{min}), particularly during winter months. This asymmetric warming pattern, characterized by stronger trends in T_{min} than in maximum temperature (T_{max}), is consistent with observed climate change across Canada, where nighttime and cold-season warming dominate long-term temperature trends [37,42]. Such warming is often attributed to increased greenhouse gas concentrations, changes in cloud cover, and snow–albedo feedback mechanisms that preferentially elevate minimum temperatures during winter [24,37]. The projected reduction in cold season temperature variability suggests fewer extreme cold events and more thermally stable winters, a pattern widely reported in regional and national climate assessments for southern Ontario and other mid-latitude regions of Canada [42,43]. However, the observed historical Tmin trend of approximately 0.033 °C per decade is consistent with warming trends reported across southern Ontario and Canada. However, the projected future winter Tmin increase of up to 0.13 °C per decade exceeds the historical rate, suggesting an acceleration of warming under future climate scenarios. Similar increases in winter temperatures have been reported in recent regional and national climate assessments. These changes have important implications for snow accumulation, freeze–thaw cycles, soil processes, and ecosystem functioning at the watershed scale.

In difference, long-term trends in mean precipitation remain weak or statistically insignificant, consistent with previous Canadian studies showing that climate change impacts on precipitation often manifest more strongly through changes in variability and extremes than through shifts in long-term averages [43,44]. The increased summer and early fall precipitation variability observed in this study, including higher variance and altered wet and dry spell characteristics, suggests a growing likelihood of short-duration, high-intensity rainfall events despite relatively stable monthly means [37]. These changes are particularly relevant for watershed management, as they may intensify flood risk, soil erosion, and nutrient transport. From a methodological perspective, the results confirm that statistical downscaling using SDSM is well suited for reproducing daily temperature characteristics and seasonal variability but exhibits greater uncertainty for precipitation, especially during convective warm-season events [45]. Nevertheless, the validated SDSM framework provides a practical and effective tool for generating locally relevant, daily time-scale climate data, supporting climate impact assessments and adaptive water resource planning in southern Ontario watersheds.

Limitations and Uncertainties

Several limitations should be considered when interpreting the results. First, the downscaling was performed using only one GCM (CGCM2) and one emissions scenario (SRES A2). Structural uncertainty (differences among climate models) and scenario uncertainty (alternative emission pathways) are therefore not quantified. Internal climate variability is partially represented through the 100-member SDSM ensemble, but this does not replace multi-model ensembles. As noted by Knutti & Sedláček [36], single-model assessments may underestimate the range of possible future conditions. Second, the validation period ends in 2001 due to data availability at the time of the study; the absence of the most recent two decades (2005–2025), the warmest on record, means that model performance under the most intense observed warming could not be tested. Third, precipitation downscaling performance is modest, particularly for warm-season extremes; therefore, quantitative projections of heavy rainfall should be treated as indicative rather than definitive. Given the modest performance of precipitation downscaling (monthly NSE as low as 0.25 although annually NSE = 0.71 as mentioned in Table S2.4 of Supplementary Material S10), projections of precipitation variability and extremes should be interpreted with caution. The observed increase in variance may be exaggerated. However, the direction of change is consistent with physical expectations under warm months in summer season. Fourth, spatial-representativeness uncertainty from using a single station is not quantified; however, the small-sized watershed and low relief minimize this concern. Future direction should consider multi-site downscaling. Despite these limitations, the directional warming signals (especially in T_{min}) and the increased summer precipitation variability are consistent with findings from more recent model ensembles [26,27], lending confidence to the overall trends.

6. Implications for Environmental and Resource Management

These projected climate changes derived from statistically downscaled CGCM2 scenarios have important implications for watershed planning and environmental resource management in southern Ontario. The identified warming signal, particularly the statistically significant increases in winter minimum temperatures and reduced cold-season variability, suggests fundamental shifts in hydrological processes that govern runoff generation, groundwater recharge, and snowpack dynamics. Warmer winters are likely to reduce snow accumulation and advance snowmelt timing, increasing the risk of mid-winter runoff events while decreasing spring freshet contributions. Such changes can alter seasonal flow regimes and place additional pressure on existing stormwater and drainage infrastructure.

Although mean monthly precipitation does not exhibit statistically significant long-term trends, the observed redistribution toward wetter summers, combined with increased precipitation variability and shortened wet-spell durations, has critical implications for water management. More episodic and intense rainfall events can increase surface runoff, soil erosion, and nutrient transport, thereby degrading water quality in agricultural and mixed-use watersheds. These conditions heighten the risk of flooding during summer storms while simultaneously increasing the likelihood of dry spells that stress crops and ecosystems during the growing season.

From an agricultural perspective, warmer growing seasons may extend crop productivity potential but also increase evapotranspiration demands, potentially reducing effective soil moisture despite stable or slightly increased summer precipitation. This dual stress underscores the need for adaptive water management strategies, such as improved soil moisture conservation, enhanced drainage control, and flexible irrigation planning. Ecosystem services, including wetland function and aquatic habitat stability, may also be affected by altered flow timing and increased hydrologic variability.

The use of statistically downscaled climate data provides a critical advantage for adaptation planning at the watershed scale. SDSM enables the translation of large-scale climate signals into locally relevant daily weather sequences, supporting impact assessments that require fine temporal resolution. For southern Ontario watersheds, such downscaled datasets offer valuable inputs for evaluating climate-resilient infrastructure design, land-use planning, and water resource management strategies under plausible future climate conditions.

7. Conclusions

This study applied SDSM to evaluate historical and future climate variability for a southern Ontario watershed using observed daily climate data and large-scale predictors from the CGCM2. The results indicate a consistent warming trend, with minimum temperature (Tmin) exhibiting the strongest increases, particularly during the winter months of December and January, reaching up to 0.13 °C per decade under future climate projections. In contrast, annual precipitation totals are projected to remain relatively stable, although increased seasonal variability and changes in precipitation distribution suggest a greater likelihood of short-duration heavy rainfall events and altered hydrological conditions. These findings indicate that future climate change in the watershed is expected to be driven primarily by increasing temperatures rather than substantial changes in total precipitation.

Historical analyses indicate limited long-term trends in mean precipitation but reveal clear temperature-warming signals, particularly in minimum temperatures. These historical patterns provide a credible baseline against which future projections were evaluated. Future predicated projections for the future period 2025–2044 indicate continued warming across all months, with statistically significant increases in winter T_{max} and T_{min} and a marked reduction in cold-season temperature variability. These changes point to fewer extreme cold events and more thermally stable winters, consistent with broader regional climate assessments.

In contrast, future mean monthly precipitation shows no statistically significant linear trends; however, important changes emerge in seasonal distribution and variability. Summer and early fall precipitation exhibits modest increases in mean values alongside higher variance and altered wet- and dry-spell characteristics. These patterns suggest an increased likelihood of heavy rainfall events occurring over shorter durations, despite stable monthly averages, though these projections should be treated as indicative rather than definitive given the modest performance of precipitation downscaling. Such changes have important implications for flood risk, soil erosion, and water quality management at the watershed scale.

Overall, the findings highlight that climate change impacts may manifest more strongly through changes in variability and extremes than through shifts in long-term means. The validated SDSM framework provides a valuable tool for generating locally relevant climate inputs for impact studies, particularly where daily-scale data are required.

Future research should extend this work by integrating downscaled climate projections with physically based hydrological and water quality models to quantify impacts on streamflow, sediment transport, and nutrient loading. Additional focus on extreme event analysis, multi-model climate ensembles, and updated emissions pathways (e.g., CMIP6 SSPs) would further strengthen uncertainty characterization and support more resilient water resource planning in southern Ontario watersheds. Future work should also apply bias correction or alternative downscaling methods (e.g., AI mapping, machine learning) to improve precipitation estimates.

Supplementary Materials: The following supporting information can be downloaded at: https://www.mdpi.com/article/10.3390/cli14070150/s1, Table S1 and S2.1–S2.4; Figures S1, S2, S3.1–S3.3, S4.1–S4.4 and S5.1–S5.6 are supporting material for this research. However, the supplementary file also includes more detailed descriptions of the methodology, specifically about the SDSM analysis for downscaled prediction used in this study (S1 to S10). The supplementary methods and data refer to references [46–51], which are included in the main manuscript's reference list.

Author Contributions: All the analyses of the data and the preparation of the manuscripts were primarily completed by R.H. and R.S. under the supervision of R.P.R. and P.G. Conceptualization, R.P.R. and P.G.; methodology, R.P.R. and P.G.; formal analysis, R.H., R.S. and A.S.; investigation, R.P.R., R.S. and P.G.; resources, P.G., R.S. and R.P.R.; water quality and field data, P.G. and A.S.; data curation, R.H. and R.S.; writing—original draft preparation, R.H. and R.S.; writing—review and editing, R.P.R., A.S., P.G. and R.S.; visualization, R.P.R., R.S. and P.G.; project administration, R.P.R. All authors have read and agreed to the published version of the manuscript.

Funding: This research received no external funding.

Institutional Review Board Statement: Not applicable.

Informed Consent Statement: Not applicable.

Data Availability Statement: The data presented in this study are available upon request from the corresponding or first author.

Acknowledgments: The authors gratefully acknowledge the Grand River Conservation Authority and the Ontario Ministry of the Environment, Conservation and Parks for providing valuable data and technical guidance that supported the methodology and approach of this study. The authors also acknowledge the School of Engineering at the University of Guelph, Ontario, Canada, for supporting this research.

Conflicts of Interest: The authors declare no conflicts of interest.

References

1. Caretta, M.A.; Mukherji, A.; Arfanuzzaman, M.; Betts, R.A.; Gelfan, A.; Hirabayashi, Y.; Lissner, T.K.; Liu, J.; Lopez Gunn, E.; Morgan, R.; et al. Water. In *Climate Change 2022: Impacts, Adaptation and Vulnerability. Contribution of Working Group II to the Sixth Assessment Report of the Intergovernmental Panel on Climate Change*; Pörtner, H.-O., Roberts, D.C., Tignor, M., Poloczanska, E.S., Mintenbeck, K., Alegría, A., Craig, M., Langsdorf, S., Löschke, S., Möller, V., et al., Eds.; Cambridge University Press: Cambridge, UK, 2022; pp. 551–712.
2. Lee, H.; Calvin, K.; Dasgupta, D.; Krinner, G.; Mukherji, A.; Thorne, P.; Trisos, C.; Romero, J.; Aldunce, P.; Barret, K.; et al. *Climate Change 2023: Synthesis Report. Contribution of Working Groups I, II and III to the Sixth Assessment Report of the Intergovernmental Panel on Climate Change*; IPCC: Geneva, Switzerland, 2023; 184p.
3. Wu, K.; Johnston, C.A. Hydrologic response to climatic variability in a Great Lakes watershed: A case study with the SWAT model. *J. Hydrol.* **2007**, *337*, 187–199. [CrossRef]
4. Yang, Q.; Meng, F.R.; Zhao, Z.; Chow, T.L.; Benoy, G.; Rees, H.W.; Bourque, C.P.-A. Assessing the impacts of flow diversion terraces on stream water and sediment yields at a watershed level using SWAT model. *Agric. Ecosyst. Environ.* **2009**, *132*, 23–31. [CrossRef]
5. Kling, G.; Hayhoe, K.; Johnson, L.B.; Magnuson, J.J.; Polasky, S.; Robinson, S.K.; Shuter, B.J.; Wander, M.M.; Wuebbles, D.J.; Zak, D.R. *Confronting Climate Change in the Great Lakes Region: Impacts on Our Communities and Ecosystems*; Union of Concerned Scientists: Cambridge, MA, USA; Ecological Society of America: Washington, DC, USA, 2003.
6. Cooke, S. *Water Quality in the Grand River: A Summary of Current Conditions (2000–2004) and Long Term Trends*; Grand River Conservation Authority: Cambridge, ON, Canada, 2006.
7. Bonsal, B.R.; Peters, D.L.; Seglenieks, F.; Rivera, A.; Berg, A. Changes in freshwater availability across Canada. In *Canada's Changing Climate Report*; Bush, E., Lemmen, D.S., Eds.; Government of Canada: Ottawa, ON, Canada, 2019; Chapter 6; pp. 261–342.
8. Ahmed, S.I.; Rudra, R.; Goel, P.; Amili, A.; Dickinson, T.; Singh, K.; Khan, A. Change in Winter Precipitation Regime across Ontario, Canada. *Hydrology* **2022**, *9*, 81. [CrossRef]
9. de Elia, R.; Cote, H. Climate and climate change sensitivity to model configuration in the Canadian RCM over North America. *Meteorol. Z.* **2010**, *19*, 325–339. [CrossRef]
10. Miele, A.; Chen, J.; Khan, A. A review of climate change impacts on hydrology and water quality in Canada: Current knowledge and future research directions. *Sci. Total Environ.* **2023**, *875*, 162653.
11. Nakicenovic, N.; Davidson, O.; Davis, G.; Grübler, A.; Kram, T.; La Rovere, E.L.; Metz, B.; Morita, T.; Pepper, W.; Pitcher, H. *IPCC Special Report on Emissions Scenarios*; Cambridge University Press: Cambridge, UK, 2000.
12. Wilby, R.L.; Dawson, C.W.; Barrow, E.M. SDSM—A decision support tool for the assessment of regional climate change impacts. *Environ. Model. Softw.* **2002**, *17*, 147–159. [CrossRef]
13. Diaz-Nieto, J.; Wilby, R.L. A comparison of statistical downscaling and climate change factor methods: Impacts on low flows in the river thames, united kingdom. *Clim. Change* **2005**, *69*, 245–268. [CrossRef]
14. Munawar, S.; Rahman, G.; Moazzam, M.F.U.; Miandad, M.; Ullah, K.; Al-Ansari, N.; Linh, N.T.T. Future Climate Projections Using SDSM and LARS-WG Downscaling Methods for CMIP5 GCMs over the Transboundary Jhelum River Basin of the Himalayas Region. *Atmosphere* **2022**, *13*, 898. [CrossRef]
15. Shukla, R.; Khare, D.; Dwivedi, A.K.; Rudra, R.P.; Palmate, S.S.; Ojha, C.S.P.; Singh, V.P. Evaluation of statistical downscaling model's performance in projecting future climate change scenarios. *J. Water Clim. Change* **2023**, *14*, 3559–3595. [CrossRef]
16. Wilby, R.L.; Dawson, C.W. *Using SDSM Version 4.2: A Decision Support Tool for the Assessment of Regional Climate Change Impacts*; Environment Canada: Ottawa, ON, Canada, 2004.
17. Wilby, R.L.; Dawson, C.W.; Yu, D.; Herring, Z.; Baruch, A.; Ascott, M.J.; Murphy, C. Spatial and temporal scaling of sub-daily extreme rainfall for data sparse places. *Clim. Dyn.* **2023**, *60*, 3577–3596.
18. Zhou, Q.; Zhong, Y.; Chen, M.; Duan, W. Climate Change Impacts on Agricultural and Industrial Water Demands in the Beijing–Tianjin–Hebei Region Using Statistical Downscaling Model (SDSM). *Water* **2023**, *15*, 4225. [CrossRef]

19. Dafouf, S.; Lahrach, A.; Tabyaoui, H.; Benaabidate, L. Future Evolutions of Precipitation and Temperature Using the Statistical Downscaling Model (SDSM), Case of the Guir and the ZizWatershed, Morocco. *Earth* **2025**, *6*, 4. [CrossRef]
20. Gagnon, S.; Singh, B.; Rousselle, J.; Roy, L. An application of the statistical downscaling model (SDSM) to simulate climate data for streamflow modelling in Quebec. *Can. Water Resour. J.* **2005**, *30*, 297–314. [CrossRef]
21. Cunderlik, J.M.; Simonovic, S.P. Hydrological extremes in a southwestern Ontario river basin under future climate conditions. *Hydrol. Sci. J.* **2005**, *50*, 631–654. [CrossRef]
22. de Elia, R.; Caya, D.; Cote, H.; Frigon, A.; Biner, S.; Giguere, M.; Paquin, D.; Harvey, R.; Plummer, D. Evaluation of uncertainties in the CRCM-simulated North American climate. *Clim. Dyn.* **2008**, *30*, 113–132.
23. Wilby, R.L. Hopes and Fears of a Climate Scientist. In Proceedings of the Sustainability and Climate Change, Sharm El-Sheikh, Egypt, 6–18 November 2022; Conference Paper. Available online: https://www.researchgate.net/publication/364956536 (accessed on 24 February 2025).
24. Bonsal, B.; Shabbar, A. *Large-Scale Climate Oscillations Influencing Canada, 1900–2008: Canadian Biodiversity: Ecosystem Status and Trends 2010*; Technical Thematic Report No. 4; Canadian Councils of Resource Ministers: Ottawa, ON, Canada, 2011; 20p.
25. Dibike, Y.B.; Coulibaly, P. Hydrologic impact of climate change in the Saguenay watershed: Comparison of downscaling methods and hydrologic models. *J. Hydrol.* **2005**, *307*, 145–163. [CrossRef]
26. Champagne, O.; Arain, M.A.; Leduc, M.; Coulibaly, P.; McKenzie, S. Future shift in winter streamflow modulated by the internal variability of climate in southern Ontario. *Hydrol. Earth Syst. Sci.* **2020**, *24*, 3077–3096. [CrossRef]
27. Arora, V.K.; Lima, A.; Shrestha, R. The effect of climate change on the simulated streamflow of six Canadian rivers based on the CanRCM4 regional climate model. *Hydrol. Earth Syst. Sci.* **2025**, *29*, 291–312. [CrossRef]
28. Thakor, H.B.; Parekh, F.P. Statistical downscaling model (SDSM) for long-term prediction of rainfall and maximum temperature. In *Innovation in Smart and Sustainable Infrastructure*; Patel, D., Kim, B., Han, D., Eds.; Springer Nature: Cham, Switzerland, 2024; pp. 477–486.
29. Challa, V.; Renganathan, M. Assessment of Climate Change Impact on Meteorological Variables of Indravati River Basin Using SDSM and CMIP6 Models. *Environ. Monit. Assess.* **2025**, *197*, 22.
30. Oogathoo, S. Runoff Simulation in the Canagagigue Creek Watershed Using the MIKE SHE Model. Master's Thesis, McGill University, Montreal, QC, Canada, 2006.
31. Das, S.; Rudra, R.P.; Gharabaghi, B.; Goel, P.K.; Singh, A.; Ahmed, I. Comparing the performance of SWAT and AnnAGNPS model in a watershed in Ontario. In *Proceedings of the 2007 ASABE Annual Meeting, Minneapolis, MN, USA, 17–20 June 2007*; ASABE: St. Joseph, MI, USA, 2007; Paper No. 072023.
32. Hoffman, D.W.; Matthews, B.C.; Wicklund, R.E. *Soil Survey of Wellington County Ontario*; Report No. 35 of the Ontario Soil Survey; Canada Department of Agriculture and Ontario Department of Agriculture: Ottawa, ON, Canada, 1963.
33. Presant, E.W.; Wicklund, R.E. *The Soils of Waterloo County*; Report No. 44 of the Ontario Soil Survey; Canada Department of Agriculture and Ontario Department of Agriculture: Ottawa, ON, Canada, 1971.
34. Zhang, X.; Srinivasan, R.; Hao, F. Predicting hydrologic response to climate change in the luohe river basin using the SWAT model. *Trans. ASABE* **2007**, *50*, 901–910. [CrossRef]
35. Canadian Climate Change Scenarios Network (CCCSN). Canadian Climate Change Scenarios Network. Available online: http://www.cccsn.ca (accessed on 28 February 2026).
36. Knutti, R.; Sedláček, J. Robustness and Uncertainties in the New CMIP5 Climate Model Projections. *Nat. Clim. Change* **2013**, *3*, 369–373. [CrossRef]
37. Masson-Delmotte, V.; Zhai, P.; Pirani, A.; Connors, S.L.; Péan, C.; Berger, S.; Caud, N.; Chen, Y.; Goldfarb, L.; Gomis, M.I.; et al. *Climate Change 2021: The Physical Science Basis: Contribution of Working Group I to the Sixth Assessment Report of the Intergovernmental Panel on Climate Change*; Cambridge University Press: Cambridge, UK, 2021; 2391p. [CrossRef]
38. Harpham, C.; Wilby, R.L. Multi-site downscaling of heavy daily precipitation occurrence and amounts. *J. Hydrol.* **2005**, *312*, 235–255. [CrossRef]
39. Environment Canada. *Canadian Daily Climate Data Conversion Utility, CDCD-Extract V1.06*; Environment Canada: Ottawa, ON, Canada, 2000.
40. Environment Canada. *Canadian Daily Climate Data, CDCD Version 1.02*; Environment Canada: Ottawa, ON, Canada, 2000.
41. Moriasi, D.N.; Arnold, J.G.; Van Liew, M.W.; Bingner, R.L.; Harmel, R.D.; Veith, T.L. Model evaluation guidelines for systematic quantification of accuracy in watershed simulations. *Trans. ASABE* **2007**, *50*, 885–900. [CrossRef]
42. Vincent, L.A.; Zhang, X.; Mekis, E.; Wan, H.; Bush, E.J. Changes in Canada's climate: Trends in indices based on daily temperature and precipitation data. *Atmos.-Ocean* **2018**, *56*, 332–349. [CrossRef]
43. Zhang, X.; Flato, G.; Kirchmeier-Young, M.; Vincent, L.; Wan, H.; Wang, X.; Rong, R.; Fyfe, J.; Li, G.; Kharin, V.V. Changes in Temperature and Precipitation Across Canada. In *Canada's Changing Climate Report*; Bush, E., Lemmen, D.S., Eds.; Government of Canada: Ottawa, ON, Canada, 2019; pp. 112–193.

44. Mekis, É.; Brown, R. Derivation of an adjustment factor map for the estimation of the water equivalent of snowfall from ruler measurements in Canada. *Atmos.-Ocean* **2010**, *48*, 284–293. [CrossRef]
45. Wilby, R.L.; Dawson, C.W. *SDSM 4.2—A Decision Support Tool for the Assessment of Regional Climate Change Impacts: User Manual*; Lancaster University and Environment Agency of England and Wales: Lancaster, UK, 2007. Available online: https://sdsm.org.uk/SDSMManual.pdf (accessed on 5 December 2024).
46. Nash- Wilby, R.L.; Wigley, T.M.L. Precipitation predictors for downscaling: Observed and general circulation model relationships. *Int. J. Climatol.* **2000**, *20*, 641–661. [CrossRef]
47. Hessami, M.; Gachon, P.; Ouarda, T.B.M.J.; St-Hilaire, A. Automated regression-based statistical downscaling tool. *Environ. Model. Softw.* **2008**, *23*, 813–834. [CrossRef]
48. Dibike, Y.B.; Coulibaly, P. Validation of hydrological models for climate scenario simulation: The case of Saguenay watershed in Quebec. *Hydrol. Process.* **2007**, *21*, 3123–3135. [CrossRef]
49. Dibike, Y.B.; Gachon, P.; St-Hilaire, A.; Ouarda, T.B.M.J.; Nguyen, V.T.V. Uncertainty analysis of statistically downscaled temperature and precipitation regimes in Northern Canada. *Theor. Appl. Climatol.* **2008**, *91*, 149–170.
50. Khan, M.S.; Coulibaly, P.; Dibike, Y. Uncertainty analysis of statistical downscaling methods. *J. Hydrol.* **2006**, *319*, 357–382. [CrossRef]
51. SYSTAT Software, Inc. *MYSTAT: A Student Version of SYSTAT 32-Bit Unicode English, Version No. 12.02*; SYSTAT Software, Inc.: San Jose, CA, USA, 2007.